

Formalizing and Evaluating Requirements of Perception Systems for Automated Vehicles using Spatio-Temporal Perception Logic

Mohammad Hekmatnejad, Bardh Hoxha, Jyotirmoy V. Deshmukh, Yezhou Yang, and Georgios Fainekos

Abstract—Automated vehicles (AV) heavily depend on robust perception systems. Current methods for evaluating vision systems focus mainly on frame-by-frame performance. Such evaluation methods appear to be inadequate in assessing the performance of a perception subsystem when used within an AV. In this paper, we present a logic – referred to as Spatio-Temporal Perception Logic (STPL) – which utilizes both spatial and temporal modalities. STPL enables reasoning over perception data using spatial and temporal relations. One major advantage of STPL is that it facilitates basic sanity checks on the real-time performance of the perception system, even without ground-truth data in some cases. We identify a fragment of STPL which is efficiently monitorable offline in polynomial time. Finally, we present a range of specifications for AV perception systems to highlight the types of requirements that can be expressed and analyzed through offline monitoring with STPL.

Index Terms—Formal Methods, Perception System, Temporal Logic, Autonomous Driving Systems.

I. INTRODUCTION

The safe operation of automated vehicles (AV), advanced driver assist systems (ADAS), and mobile robots in general, fundamentally depends on the correctness and robustness of the perception system (see discussion in [1] section 5). Faulty perception systems and, consequently, inaccurate situational awareness can lead to dangerous situations [2], [3]. For example, in the accident in Tempe in 2018 involving an Uber vehicle [2], different sensors had detected the pedestrian, but the perception system was not robust enough to assign a single consistent object class to the pedestrian. Hence, the AV was not able to predict the future path of the pedestrian. This accident highlights the importance of identifying the right questions to ask when evaluating perception systems.

In this paper, we argue that in order to reduce the likelihood of future accidents, we need to be able to formally express what should be the assumptions, performance, and guarantees provided by a perception system. For instance, the aforementioned accident highlights the need for predicting the right object class quickly and robustly. An informal requirement

(in natural language) expressing such a perception system performance expectation could be:

Req. 1: Whenever a new object is detected, then it is assigned a class within 1 sec, after which the object does not change class until it disappears.

A sequence of six image frames from the KITTI dataset is shown in Figure 1. All detected objects with bounding boxes are labeled with class names such as *Car*, *Pedestrian*, and *Cyclist* in those frames. Nonetheless, in Fig. 1(a), a *cyclist* that was detected in frame $f = 0$ and existed in frame $f = 1$ changed its class to *pedestrian* in frame $f = 2$, which is a violation of Req. 1. If such a requirement is too strict for the capabilities of the perception system, then it could be relaxed by requiring that the object is properly classified in at least 4 out of 5 frames (or any other desired frequency). The first challenge for an automated testing/validation/verification system is to be able to formally (i.e., mathematically) represent such high-level requirements.

Formalizing the expectations on the performance of the perception system has several benefits. First and foremost, such requirements can help us evaluate AV/ADAS perception systems beyond what existing metrics used in vision and object tracking can achieve [6], [7]. In particular, evaluation metrics used for image classification algorithms are operating on a frame-by-frame basis ignoring cross-frame relations and dependencies. Although tracking algorithms can detect misclassifications, they cannot assess the frequency and severity of them. For example, misclassifying a car as a static object could lead to severe consequences.

Second, formal specifications enable automated testing and monitoring for AV, e.g., see [8]–[15], for requirements based testing. Third, formal specifications on the perception system can also function as a requirements language between original equipment manufacturers (OEM) and suppliers. As a simple example for the need of a requirements language consider the most basic question: should the image classifier correctly classify all objects within the sensing range of the lidar, or all objects of at least x pixels in diameter? Again, *without requirements, any system behavior is acceptable and, most importantly, not testable/verifiable!* Finally, using a formal specification language, we can search offline perception datasets to find scenarios that violate the requirements in order to reproduce them in simulation, e.g., [16].

Works like [10] and [12] demonstrated the importance of testing system level requirements for an AV when the AV contains machine learning enabled perception components.

Mohammad Hekmatnejad was with the School of Computing and Augmented Intelligence (formerly CIDSE), Arizona State University, USA; e-mail: mhekmatn@asu.edu.

Bardh Hoxha is with the Toyota Research Institute of North America, USA.

Jyotirmoy V. Deshmukh is with the University of Southern California, USA.

Yezhou Yang is with Arizona State University, USA.

Georgios Fainekos is with the Toyota Research Institute of North America, USA; the work was performed while he was with the Arizona State University, USA.

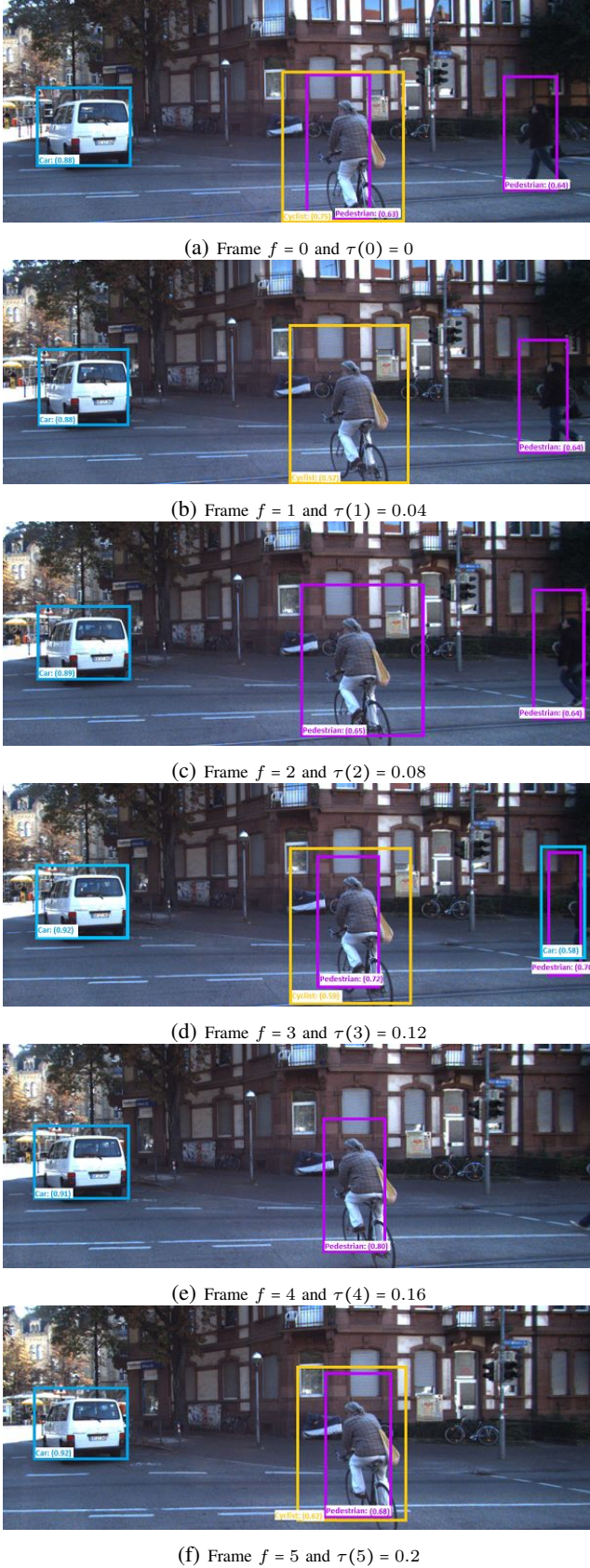


Fig. 1: A series of image frames taken from KITTI [4] augmented with the data about classified data-objects using SqueezeDet [5]. Here, τ is a function that maps each frame to its captured time.

However, Signal Temporal Logic (STL) by [17] used in [10] and [12] cannot directly express requirements on the performance of the perception system itself. This limitation was identified in [18] and a new logic – Timed Quality Temporal Logic (TQTL) was developed, which can directly express requirements for image classification algorithms like SqueezeDet by [5]. TQTL is based on Timed Propositional Temporal Logic (TPTL) [19] and it allows reasoning over objects classified in video frames. For example, TQTL can formalize Req. 1 that an object should not change classes, but it does not support spatial or topological reasoning over the objects in a scene. This is a major limitation since TQTL cannot express requirements such as occlusion, overlap and other spatial relations for basic sanity checks, e.g., that objects do not teleport from frame to frame. In addition, one cannot query databases for events such as “a motorbike passing a truck on the left within 2 sec”.

In this paper, we introduce the Spatio-Temporal Perception Logic (STPL) which expands TQTL with operators from the spatial logic $S4_u$ [20]. When the spatial logic $S4_u$ is combined with Linear Temporal Logic (LTL) [21] or STL, it enables set based operations over time modalities (e.g., see [22], [23]). From a different perspective, we expand prior results on spatio-temporal logics [22], [23] with object quantifiers, freeze time operators, functions and other topological operators. For example with STPL, we can express requirements such as:

Req. 2: The frames per second of the camera is high enough so that for all detected cars, their bounding boxes self-overlap for at least 3 frames and for at least 10% of the area. which is satisfiable for the image frames in Fig. 1.

Beyond the previous examples, we need tools to assess the performance of new machine learning components for AV/ADAS. For example, STPL could assess how rain removal algorithms (see the work by [24]) improve the performance of the object detection algorithms over video streams. As another example, STPL could evaluate the impact of a point cloud clustering algorithm on a prediction algorithm [25], [26]). Since STPL needs to refer to, reason and compare objects at different points in time, our foundational logic of time is TPTL [19]. Unfortunately, the time complexity of monitoring TPTL requirements is PSPACE-hard [27]. Hence, we work with TPTL fragments that are efficiently computable [28], [29].

In summary, STPL

- extends TQTL by enabling spatial reasoning through functions and relations;
- extends $LTL \times S4_u$ set-based reasoning by enabling efficient offline monitoring tools;
- targets the analysis of perception systems; and
- is supported by open source monitoring tools [30].

We further envision that our tools can be used for applications beyond ADAS/AV. For example, in robot manipulation problems where mission requirements are already described in temporal logic (e.g., see [31] and [32]).

A. Related Works

Logics about topology and space have a long history going as far back as 1989 (see [33]). Region Connection Calculus

[34], Shape Calculus [35], and Situation Calculus [36] are just some examples of the vast literature. Comprehensive surveys and comparisons of reasoning methods about topology and time are provided [20], [37]. Spatio-temporal logics and calculi are also frequently used in robotics for human-robot communication [38], [39] and for specifying and verifying properties of AV [40], [41]. All the aforementioned works that deal with topology and time primarily focus on deductive reasoning, theorem proving, knowledge representation, axiomatization, and – in some cases – planning.

However, STPL requires computationally efficient tools for spatio-temporal reasoning in order to monitor data streams from perception systems. Even though there exist spatio-temporal logics that can process streaming data (offline or online), e.g., SpaTeL [42], SSSL [43], or SaSTL [44] (for a short survey see [45]), or even images, e.g., SLCS [46], all these logics are application dependent and cannot support the topological reasoning needed for perception data in AV.

In another work, a graph-based spatio-temporal logic GSTL [47] is presented for knowledge representation and reasoning. GSTL deals with spatial elements as regions, and uses *mereotopology* (combination of *mereology* and *topology* to support parthood and connectivity, respectively) to represent relations between spatial elements. It exploits rectangle/cubic algebra to represent spatial objects. GSTL combines STL temporal logic with mereotopology-based spatial operators enriched with interval algebra. The satisfiability problem for GSTL is decidable by restricting the evolution of spatial elements.

In the following, we highlight major differences of SpaTeL and SSSL logics in comparison with STPL. We exclude GSTL in our comparison mainly because it was primarily designed for model checking which restricts its expressivity for decidability reasons.

The two spatio-temporal languages SSSL [43] and SpaTeL [42] are explicitly developed for describing high-level spatial patterns that evolve. Both languages are founded based on a graph-based representation of discrete models of space. For the SSSL, undirected weighted graphs are used to model space, and in SpaTeL, a networked system whose states encapsulate an image are represented as quad transition systems.

In SSSL, the syntax of the language adds two spatial operators $\Diamond_{[w_1, w_2]} \varphi$ and $\varphi_1 S_{[w_1, w_2]} \varphi_2$ into STL, which are named bounded somewhere and bounded surround, respectively. The first operator requires φ to hold in a location that can be reached from the current location with a cost between w_1 and w_2 . The cost is usually the distance between the two locations. For the second operator, the notation of external boundary of a set is required. An external boundary of a given set of nodes is defined as the set of nodes that are directly connected to the elements of the given set but are not members of it. The semantics of the second operator requires that for the current location l and a given trace x , l belongs to a set of locations A that all satisfy the formula φ_1 , and for all the locations in the external boundary of A , they satisfy the formula φ_2 . An SSSL formula can be arbitrarily nested.

In SpaTeL, a combination of Tree Spatial Superposition Logic (TSSL) and STL is proposed to reason on spatial

patterns. TSSL uses the quad-trees to represent the space by partitioning the space recursively into quadrants [48]. The TSSL logic is similar to the classic Computation Tree Logic (CTL) (e.g., see [49]), with the main difference that the next and until operators are not temporal, but spatial. That is, evolution happens by a change of resolution (or zoom in). All the spatial operators are augmented by a set B that selects the spatial directions (i.e., NW, NE, SW, and SE) in which the operators are allowed to work. Additionally, similar to temporal operators, there is a parameter k that limits the operator's evaluation range on a finite sequence of states. For example, $\exists_B \varphi_1 U_k \varphi_2$ means that there exists a set of directions in B by which the i -th label of a path π^B ¹ satisfies the formula φ_2 and all the other labels on the path until i satisfy the formula φ_1 . A difference between the former and the latter is that in the former one, the TSSL fragment of a formula does not include temporal subformulas. In summary, the key differences of these logics with our proposed STPL logic are:

- *Modeling*: SSSL and SpaTeL are not designed to model physical objects in 2D or 3D spaces. On the other hand, our logic is explicitly designed to handle physical objects.
- *Expressivity*: SpaTeL is inherently less expressive than SSSL due to its modeling and traversing approach on quad-trees and the decoupled syntax for spatial and temporal formulas. Therefore, we are going to compare STPL with SSSL. There are two significant differences. The first one is the presence of time freeze operator and time variables and, hence, STPL is more expressive. The second one is the presence of the quantifiers and set operations over spatial terms/locations. As an example, SSSL cannot reason on whether the same object over two different frames overlaps or not with itself.
- *Application*: SSSL and SpaTeL are mostly helpful for pattern recognition purposes, while STPL is a more general-purpose language. Quantitative semantics: there is quantitative and qualitative semantics for SSSL and SpaTeL, but currently, we only presented qualitative semantics for STPL. The graph-based modeling of the spatial environment and the fixed metric properties such as distance makes it more straightforward to define quantitative semantics for their underlying logic.

More recently, the language Scenic by [50] has been developed for creating single scene images for testing object detection and classification algorithms. However, our work is complementary to languages that generate static scenes.

Therefore, our approach diverges from prior work in scope, semantics, and algorithmic details.

II. PRELIMINARIES

We start by introducing definitions that are used throughout the paper for representing classified data generated by perception subsystems. In the following, an ego car (or the Vehicle Under Test – VUT) is a vehicle equipped with perception

¹A path is a sequence of state's labels that are reachable by using the move directions, where $i \leq k$ is an order of a label on the path.

systems and other automated decision making software components, but not necessarily a fully automated vehicle (e.g., SAE automation level 4 or 5).

A. Data-object Stream

A *data-object stream* \mathcal{D} is a sequence of data-objects representing objects in the ego vehicle's environment. We refer to each dataset in the sequence as a frame. In each frame, objects are classified and stored in a data-object. Data-objects are abstract because in the absence of a standard classification format, the output of different perception systems are not necessarily compatible with each other. To simplify the presentation, we will also refer to the order of each frame in the data stream as a frame number. For each frame i , $\mathcal{D}(i)$ is the set of data-objects for frame i , where i is the order of the frame in the data-object stream \mathcal{D} . We assume that a data stream is provided by a perception system, in which a function \mathcal{R} retrieves data-attributes for an identified object. A *data-attribute* is a property of an object such as class, probability, geometric characteristics, etc. Some examples could be:

- by $\mathcal{R}(\mathcal{D}(i), ID).Class$, we refer to the class of an object identified by ID in the i 'th frame,
- by $\mathcal{R}(\mathcal{D}(i), ID).Prob$, we refer to the probability that an object identified by ID in the i 'th frame is correctly classified,
- by $\mathcal{R}(\mathcal{D}(i), ID).PC$, we refer to the point clouds associated with an object identified by ID in the i 'th frame.

The function \mathcal{OI} returns the set of identifiers for a given set of data-objects. By $\mathcal{OI}(\mathcal{D}(i))$, we refer to all the identifiers that are assigned to the data-objects in the i 'th frame. Another important attribute of each frame is its time stamp, i.e., when this frame was captured in physical time. We represent this attribute for the frame i by $\tau(i)$.

Example 1: Assume that data-object stream \mathcal{D} is represented in Figure 1, then the below equalities hold:

- $\mathcal{OI}(\mathcal{D}(1)) = \{1, 2, 3\}$
- $\mathcal{OI}(\mathcal{D}(1), 2).Class = cyclist$
- $\mathcal{OI}(\mathcal{D}(1), 2).Prob = 0.57$
- $\tau(1) = 0.04$

B. Topological Spaces

Throughout the paper, we will be using \mathbb{N} to refer to the set of natural numbers and \mathbb{R} to real numbers. In the following, for completeness, we present some definitions and notation related to topological spaces and the $S4_u$ logic which are adopted from [22] and [51]. Later, we build our $MTL \times S4_u$ definition on this notation.

Definition 2.1 (Topological Space): A topological space is a pair $\mathcal{T} = \langle \mathbb{U}, \mathbf{I} \rangle$ in which \mathbb{U} is the universe of the space, and \mathbf{I} is the interior operator on \mathbb{U} . The universe is a nonempty set, and \mathbf{I} satisfies the standard Kuratowski axioms:

$$\mathbf{I}(X \cap Y) = \mathbf{I}X \cap \mathbf{I}Y, \mathbf{I}X \subseteq \mathbf{I}\mathbf{I}X, \mathbf{I}X \subseteq X, \text{ and } \mathbf{I}\mathbb{U} = \mathbb{U}.$$

We denote \mathbf{C} (closure) as the dual operator to \mathbf{I} , such that $\mathbf{C}X = \mathbb{U} - \mathbf{I}(\mathbb{U} - X)$ for every $X \subseteq \mathbb{U}$. Below we list some remarks related to the above definitions:

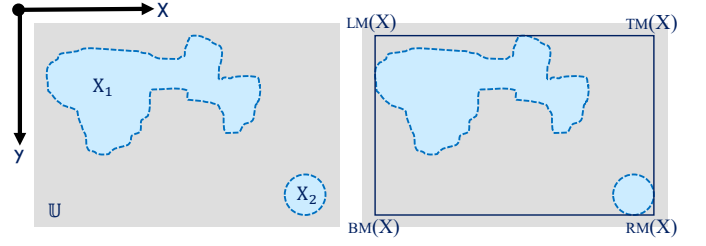


Fig. 2: Let $X = X_1 \cup X_2$ with $\mathbf{C}X = X$. Left: the whole rectangle represents the universe (colored gray) \mathbb{U} , the regions X_1 and X_2 without the dashed-lines (colored light blue) represent the interior $\mathbf{I}X$ of the set X , the dashed lines (colored darker blue) represent the boundary $\mathbf{C}X - \mathbf{I}X$ of the set X , and the remaining region represents $\mathbb{U} - X$. Right: the bounding box around set X with four corners named as in Def. 2.3.

- $\mathbf{I}X$ is the *interior* of a set X ,
- $\mathbf{C}X$ is the *closure* of a set X ,
- X is called *open* if $X = \mathbf{I}X$,
- X is called *closed* if $X = \mathbf{C}X$,
- If X is an open set then its complement $\overline{X} = \mathbb{U} - X$ is a closed set and vice versa,
- For any set $X \subseteq \mathbb{U}$, its *boundary* is defined as $\mathbf{C}X - \mathbf{I}X$ (X and its complement have the same boundary),
- By *spatial terms*, we refer to subsets of topological spaces and by *spatial variables*, we refer to propositional variables of *spatial terms* in topological spaces.

C. Image Space Notation and Definitions

Even though our work is general and applies to arbitrary finite dimensional spaces, our main focus is on 2D and 3D spaces as encountered in perception systems in robotics. In the following, the discussion focuses on 2D image spaces with the usual pixel coordinate systems. In Figure 2 left, a closed set is illustrated as the light blue region, while its boundary is a dashed-line in darker blue.

Definition 2.2 (Totally-ordered Topological Space): A Totally-ordered (TO) topological space \mathcal{S} is a topological space $\langle \mathbb{U}, \mathbf{I} \rangle$ that is equipped with a total ordering relation $\leq \subseteq \mathcal{S} \times \mathcal{S}$. That is, $\forall p_1, p_2 \in \mathcal{S}$ either $p_1 \leq p_2$ or $p_2 \leq p_1$.

Definition 2.3 (Total order in 2D spaces): In a two-dimensional (2D) TO topological space \mathcal{S} , $p = (x, y) \in \mathcal{S}$ denotes its coordinates in the x - y Cartesian coordinate system, where $x, y \in \mathbb{R}_{\geq 0}$. For $p_1 = (x_1, y_1)$, $p_2 = (x_2, y_2)$ the ordering relation is defined as:

$$(x_1, y_1) \leq_{2D} (x_2, y_2) \iff y_1 < y_2 \vee (y_1 = y_2 \wedge x_1 \leq x_2).$$

Note that even though Def. 2.3 considers the coordinates over the reals, i.e., $\mathbb{R}_{\geq 0}^2$, in practice, the image space is defined over the integers, i.e., \mathbb{N}^2 (pixel coordinates). The topological space in Figure 2 consists of the universe which is all the pixels that belong to the whole 2D gray-rectangle and the closure operator that for any set of regions includes their edges. Assume that the left-upper corner of the image is the origin of the x - y Cartesian coordinate system, and the x -axis

and the y -axis are along the width and height of the image, respectively. This is the standard coordinate system in image spaces. Then, any pixel that belongs to the universe has an order with respect to the other pixels. For example, consider $X = X_1 \cup X_2$ in Fig. 2, then all the pixels that belong to X_2 have higher orders than those in X_1 .

Definition 2.4 (Spatial Ordering Functions): Given a set S from a 2D TO topological space $\mathfrak{T} = \langle \mathbb{U}, \mathbf{I} \rangle$, we define the top-most, bottom-most, left-most, and right-most functions by $\text{TM}, \text{BM}, \text{LM}, \text{RM} : 2^{\mathbb{U}} \rightarrow 2^{\mathbb{U}}$, respectively such that

$$\begin{aligned} \text{TM}(S) &= \{p = (x_p, y_p) \mid \forall s = (x_s, y_s) \in S, \\ &\quad y_p < y_s \vee (y_p = y_s \wedge x_p \geq x_s)\} \\ \text{BM}(S) &= \{p = (x_p, y_p) \mid \forall s = (x_s, y_s) \in S, \\ &\quad y_p > y_s \vee (y_p = y_s \wedge x_p \leq x_s)\} \\ \text{LM}(S) &= \{p = (x_p, y_p) \mid \forall s = (x_s, y_s) \in S, \\ &\quad x_p < x_s \vee (x_p = x_s \wedge y_p \leq y_s)\} \\ \text{RM}(S) &= \{p = (x_p, y_p) \mid \forall s = (x_s, y_s) \in S, \\ &\quad x_p > x_s \vee (x_p = x_s \wedge y_p \geq y_s)\} \end{aligned}$$

In Def. 2.4, the notation 2^S for a set S denotes the set of all subsets of S . The right rectangle in Figure 2 shows the $\text{LM}(X)$, $\text{TM}(X)$, $\text{RM}(X)$, and $\text{BM}(X)$ points which correspond to four corners of the tightest bounding box for the set X . These sets are always singletons and therefore informally we treat them as functions that return a point.

D. Spatio-Temporal Logic $\text{MTL} \times S4_u$

Next, we introduce the logic $\text{MTL} \times S4_u$ which is a combination of Metric Temporal Logic (MTL) [52] with the $S4_u$ logic of topological spaces. It is an extension to the logic $\text{PTL} \times S4_u$ (see [22]) by adding time/frame intervals into the spatio-temporal operators. Even though $\text{MTL} \times S4_u$ is a new logic introduced in this paper, we present it in the preliminaries section since the addition of timing constraints to the syntax and semantics of PTL is straightforward.

Definition 2.5 (Syntax of $\text{MTL} \times S4_u$ as a temporal logic of topological spaces): Let Π be a finite set of spatial variables over $\mathfrak{T} = \langle \mathbb{U}, \mathbf{I} \rangle$, then a formulas φ of $\text{MTL} \times S4_u$ can be defined as follows:

$$\begin{aligned} \varphi &::= \exists \mathfrak{T} \mid \neg \varphi \mid \varphi \wedge \varphi \mid \varphi \mathcal{U}_{\mathcal{I}} \varphi \\ \mathcal{T} &::= p \mid \overline{\mathcal{T}} \mid \mathcal{T} \sqcap \mathcal{T} \mid \mathbf{I} \mathcal{T} \mid \mathcal{T} \mathcal{U}_{\mathcal{I}}^s \mathcal{T} \mid \bigcirc_{\mathcal{I}}^s \mathcal{T} \end{aligned}$$

where $p \in \Pi$ is a spatial variable.

In the above definition, the grammar for $\text{MTL} \times S4_u$ consists of two production rules φ and \mathcal{T} . In the first rule (φ), except for the *spatially exists* \exists , the other operators are the same as in MTL. That is \neg, \wedge , and $\mathcal{U}_{\mathcal{I}}$ are negation, conjunction and timed until operators, respectively (see the review by [35]). Here, the subscript \mathcal{I} denotes a non-empty interval of $\mathbb{R}_{\geq 0}$ and captures any timing constraints for the until operator. Informally, spatially exists checks whether a set has any points in it (emptiness check). Hence, the expression $\exists \mathfrak{T}$ can be viewed as an atomic proposition in MTL semantics.

The second rule (\mathcal{T}) denotes a mix of spatial and temporal operators, where p is a spatial predicate, $\overline{\mathcal{T}}$ is the spatial

complement of the spatial term \mathcal{T} , \sqcap is the spatial intersection operator, and \mathbf{I} is the spatial interior operator.

We refer to the spatio-temporal operators $\mathcal{U}_{\mathcal{I}}^s$ and $\bigcirc_{\mathcal{I}}^s$, as *Spatio-Temporal Evolving* (STE) operators. Also, we call a formula STE if it has STE operators in it. Similarly, we call a spatio-temporal formula *Spatial Purely Evolving* (SPE) if there is no STE operator in the formula. For more information refer to the (OC) and (PC) definitions by [22]. Typically, temporal logics (e.g., Metric (MTL) or Signal Temporal Logic (STL) ([35])) enable quantitative reasoning over continuous or discrete time.

In the following, we define bounded time semantics for $\text{MTL} \times S4_u$. The definition uses the spatial semantics of $S4_u$ while extends the temporal fragment (PTL) with time constraints over finite traces as in MTL. The semantics are defined over a data-object stream \mathcal{D} . However, for consistency with $\text{PTL} \times S4_u$, we will assume the existence of a spatio-temporal valuation function $\mathfrak{U} : \Pi \times \mathbb{N} \rightarrow P(\mathbb{U})$ that associates with every variable p and time frame i a subset of the topological space. In the definition of STPL, these sets will correspond to identified objects in the environment. Here, are just arbitrary subsets of the universe.

Definition 2.6 (Quantified Topological Temporal Model and Valuation): A quantified topological temporal model is a tuple of the form $\mathfrak{M} = \langle \mathfrak{T}, \mathfrak{U}, \mathcal{D}, \tau \rangle$, where $\mathfrak{T} = \langle \mathbb{U}, \mathbf{I} \rangle$ is a TO topological space, \mathfrak{U} is a spatio-temporal valuation function, \mathcal{D} is a data-object stream, $\tau : \mathbb{N} \rightarrow \mathbb{R}^+$ does mapping from frame numbers to their physical times, \mathcal{I} is any non-empty interval of $\mathbb{R}_{\geq 0}$ over time. The valuation $\mathfrak{M}(p, \mathcal{D}, i, \tau)$ represents a subset of the topological space \mathfrak{T} that is occupied by spatial variable $p \in \Pi$ in the i 'th frame (e.g., $\tau(i)$ is the captured time). The valuation \mathfrak{M} is inductively extended to any formulas that can be produced by the production rule \mathcal{T} in the Def. 2.5 as follows:

$$\begin{aligned} \mathfrak{M}(p, \mathcal{D}, i, \tau) &:= \mathfrak{U}(p, i) \\ \mathfrak{M}(\mathcal{T}_1 \mathcal{U}_{\mathcal{I}}^s \mathcal{T}_2, \mathcal{D}, i, \tau) &:= \bigcup_{i' \in \{j \in \mathbb{N} \mid \tau(j) \in (\tau(i) + \mathcal{I})\}} \left(\mathfrak{M}(\mathcal{T}_2, \mathcal{D}, i', \tau) \cap \bigcap_{i \leq i'' < i'} \mathfrak{M}(\mathcal{T}_1, \mathcal{D}, i'', \tau) \right) \\ \mathfrak{M}(\bigcirc_{\mathcal{I}}^s \mathcal{T}, \mathcal{D}, i, \tau) &:= \begin{cases} \mathfrak{M}(\mathcal{T}, \mathcal{D}, i+1, \tau) & \text{if } i+1 \in \mathbb{N}, \tau(i+1) \in (\tau(i) + \mathcal{I}) \\ \emptyset & \text{otherwise (i.e., an empty set)} \end{cases} \\ \mathfrak{M}(\mathcal{T}_1 \sqcap \mathcal{T}_2, \mathcal{D}, i, \tau) &:= \mathfrak{M}(\mathcal{T}_1, \mathcal{D}, i, \tau) \cap \mathfrak{M}(\mathcal{T}_2, \mathcal{D}, i, \tau) \\ \mathfrak{M}(\overline{\mathcal{T}}, \mathcal{D}, i, \tau) &:= \overline{\mathfrak{M}(\mathcal{T}, \mathcal{D}, i, \tau)} \\ \mathfrak{M}(\mathbf{I} \mathcal{T}, \mathcal{D}, i, \tau) &:= \mathbf{I} \mathfrak{M}(\mathcal{T}, \mathcal{D}, i, \tau) \\ \mathfrak{M}(\exists \mathfrak{T}, \mathcal{D}, i, \tau) &:= \begin{cases} \top & \text{if } \mathfrak{M}(\mathcal{T}, \mathcal{D}, i, \tau) \neq \emptyset \\ \perp & \text{otherwise (i.e., an empty set)} \end{cases} \end{aligned}$$

where $i + \mathcal{I} = \{i'' \mid \exists i' \in \mathcal{I}. i'' = i + i'\}$.

The only allowed terminals in the above syntax are \emptyset (i.e., an empty set), \mathbb{U} (i.e., the universe), and p . Here, p is a spatial invariant that function \mathfrak{U} takes in addition to a frame number and returns a subspace associated with them.

To analyze perception systems, we need to enable reasoning over both time representations, i.e., over both the frames in a data stream and the time stamps of the frames. $\mathcal{U}_{\mathcal{I}}^s$ is the

spatio-temporal until operator over time interval \mathcal{I} (e.g., $\mathcal{I} = [0, 0.2]$ includes all the time stamps that are assigned to the image frames in Figure 1), $\odot_{\mathcal{I}}^s$ is the spatio-temporal next operator over time interval \mathcal{I} . In some context, it is easier to formalize a requirement using frame intervals and reason over frames rather than time intervals. To highlight this, we add a tilde on top of the spatio-temporal operators with frame intervals, that is in $\tilde{\mathcal{U}}_{\mathcal{I}}^s$ and $\tilde{\odot}_{\mathcal{I}}^s$ the interval \mathcal{I} is over frame interval. When reasoning over frames, then $\tau(i)$ is equals to i , i.e., τ is the identity function.

In $MTL \times S4_u$, for spatial terms \mathcal{T} , \mathcal{T}_1 , and \mathcal{T}_2 , we define

- $\Box \mathcal{T} \equiv \neg \Box \neg \mathcal{T}$,
- $\mathcal{T}_1 \sqcup \mathcal{T}_2 \equiv \overline{\mathcal{T}_1} \cap \overline{\mathcal{T}_2}$,
- $\mathbf{C} \mathcal{T} \equiv \mathbf{I} \overline{\mathcal{T}}$,
- $\diamond_{\mathcal{I}}^s \mathcal{T} \equiv \bigcup \mathcal{U}_{\mathcal{I}}^s \mathcal{T}$ (Spatial-Eventually \mathcal{T} in time interval \mathcal{I}),
- $\square_{\mathcal{I}}^s \mathcal{T} \equiv \overline{\diamond_{\mathcal{I}}^s \overline{\mathcal{T}}}$ (Spatial-Always \mathcal{T} in interval \mathcal{I}),
- $\mathcal{T}_1 \mathcal{R}_{\mathcal{I}}^s \mathcal{T}_2 \equiv \overline{\mathcal{T}_1} \mathcal{U}_{\mathcal{I}}^s \overline{\mathcal{T}_2}$ (\mathcal{T}_1 Spatial-Release \mathcal{T}_2 in time interval \mathcal{I}).

using syntactic manipulation.

The same way we define equivalences of temporal operators with time-intervals, we can define equivalences for spatio-temporal operators with frame-intervals. Additionally, when we do not specify time and frame intervals for the STE operators, then $\mathcal{I} = [0, +\infty)$.

III. PROBLEM DEFINITION

Given a data stream \mathcal{D} as defined in II-A that classifies objects as set of points, the goal of this paper is to:

- 1) formulate object properties in such a data stream, and
- 2) monitor satisfiability of formulas over the stream.

A. Assumptions

Given a data stream \mathcal{D} , we assume that a tracking perception algorithm uniquely assigns identifiers to classified objects for all the frames (see the work by [53]).

In order to relax this assumption, we need to enable probabilistic reasoning within the spatio-temporal framework, which is out of the scope of this work. However, our framework could do some basic sanity checks about the relative positioning of the objects during a series of frames to detect misidentified objects.

This assumption is only needed for some certain types of requirements and for the rest it can be lifted.

B. Overall Solution

We define syntax and semantics of Spatio-Temporal Perception Logic (STPL) over sets of points in topological space, and quantifiers over objects. We build a monitoring algorithm over TPTL, MTL, and $S4_u$ and show the practicality, expressivity and efficiency of the algorithm by presenting examples. This is a powerful language and monitoring algorithm with many applications for verification and testing of complex perception systems. Our proposed language and its monitoring algorithm are different than prior works as we discussed in the introduction, and briefly listed below. STPL:

- reasons over spatial and temporal properties of objects through functions and relations;
- extends the reasoning of prior set-based logics by equipping them with efficient offline monitoring algorithm tools;
- focused on expressing and reasoning perception systems; and
- is supported by open source monitoring tools.

IV. SPATIO-TEMPORAL PERCEPTION LOGIC

In this section, we represent the syntax and semantics of the Spatio-Temporal Perception Logic.

Our proposed logic concerns the geometric properties of objects in a data stream and their evolution based on the formerly introduced definitions. Theoretically, any set-based topological space can be used in our logic. However, we restrict our topological spaces and geometric operations based on targeting problems and applications.

Next, we are going to define and interpret STPL formulas over data-object streams. We define our topological space to be axis aligned boxes in 2D images, or polyhedral sets in 3D environments. An axis aligned box is a set of two points that represent two non-adjacent corners of a box with four sides each parallel to an axis. A polyhedral is a set formed by the intersection of a finite number of closed half spaces. That is, in a data-object, $\mathcal{R}(\mathcal{D}(i), id).CS$ denotes a rectangular convex-polygon that is associated with an object id in the i 'th frame by the perception system. Similarly, $\mathcal{R}(\mathcal{D}(i), id).CS$ denotes a convex-polyhedron in the system. Without loss of generality, we are going to define the rest of the definitions for 2D images, and later in the case study, we will use bounding volumes to refer to 3D point cloud data.

A. STPL Syntax

Definition 4.1 (STPL Syntax for Discrete-Time Signal): Assume that $x \in V_t$ is a time variable, $id \in V_o$ is an ID variable, \mathcal{I} is any non-empty interval of $\mathbb{R}_{\geq 0}$ over time. The syntax for Spatio-Temporal Perception Logic (STPL) formulas is provided by the following grammar:

$$\begin{aligned} \phi ::= & \top \mid \exists id @ x. \phi \mid \neg \phi \mid \phi \vee \phi \mid \odot \phi \mid \phi \mathcal{U} \phi \mid \\ & \tau - x > t \mid \mathcal{F} - x > n \mid \mathcal{F} - x \% c > n \\ id ::= & id \mid \Theta \mid \Box \mathcal{T} \mid \mathcal{A} \end{aligned}$$

$$\begin{aligned} \mathcal{T} ::= & \mathcal{C}(id) \mid \overline{\mathcal{T}} \mid \mathcal{T} \cap \mathcal{T} \mid \mathbf{I} \mathcal{T} \mid \\ & \mathcal{T} \mathcal{U}_{\mathcal{I}}^s \mathcal{T} \mid \odot_{\mathcal{I}}^s \mathcal{T} \end{aligned}$$

$$\mathcal{A} ::= Area(\mathcal{T}) \geq r \mid Area(\mathcal{T}) \geq r \times Area(\mathcal{T})$$

$$\begin{aligned} \Theta ::= & Dist(id, CRT, id, CRT) \geq r \mid \\ & Lat(id, CRT) \geq r \mid Lon(id, CRT) \geq r \mid \\ & Lat(id, CRT) \geq r \times Lat(id, CRT) \mid \\ & Lon(id, CRT) \geq r \times Lon(id, CRT) \mid \\ & Lat(id, CRT) \geq r \times Lon(id, CRT) \mid \end{aligned}$$

$$\begin{aligned}
&Area(id) \geq r \mid Area(id) \geq r \times Area(id) \mid \\
&C(id) == c \mid C(id) == C(id) \mid P(id) \geq r \mid \\
&P(id) \geq r \times P(id)
\end{aligned}$$

$$CRT ::= LM \mid RM \mid TM \mid BM \mid CT$$

where $i \geq 0$, and the grammar starts from ϕ . Here, $\mathcal{C} : V_o \rightarrow \Pi$ is a variant-mapping function that maps object variables into spatial variables.

The time, frame and ID constraints of STPL formulas are in the form of $\tau - x > r$, $\mathcal{F} - f > n$, and $id == id$, respectively. We denote $\tau - x$ and $\mathcal{F} - x$ to refer to the elapsed time and frames, respectively. Note that we use the same variable to refer to the freeze time and frame, but distinguish their type based on how they are used in the constraints (τ represents the current time, and \mathcal{F} represents the current frame number). The freeze time quantifier, that is the x . part of $\exists id @ x. \phi$, assigns the current frame number i to variable x before processing the subformula ϕ . The prefix $\exists id$ of the $\exists id @ x. \phi$ is the *Existential ID* quantifier, and it assigns a value to the ID variable (i.e., in a frame that its number is stored in x). Similarly, the *Universal ID* quantifier is defined as $\forall id @ x. \phi \equiv \neg(\exists id @ x. \neg \phi)$. For STPL formulas ψ , ϕ , we define $\psi \wedge \phi \equiv \neg(\neg \psi \vee \neg \phi)$, $\perp \equiv \neg \top$ (False), $\psi \rightarrow \phi \equiv \neg \psi \vee \phi$ (ψ Implies ϕ), $\phi \mathcal{R} \psi \equiv \neg(\neg \phi \mathcal{U} \neg \psi)$ (ϕ releases ψ), $\phi \overline{\mathcal{R}} \psi \equiv \phi \mathcal{R} (\phi \vee \psi)$ (ϕ non-strictly releases ψ), $\diamond \psi \equiv \top \mathcal{U} \psi$ (Eventually ψ), $\Box \psi \equiv \neg \diamond \neg \psi$ (Always ψ) using syntactic manipulation.

Remark 4.2: With a slight abuse of notation, we use the *existential quantifier* $\exists id. \phi$ when there is no need for freeze time operator in *quantifier/freeze time* operator (e.g., $\exists id @ x. \phi$). Similarly, we use *freeze time* operator $x. \phi$ when there is no need for quantifiers in the *quantifier/freeze time* operator. In all the forms of the above formulas, we call the operators that precede with “.” *variant-quantifier* operators.

Definition 4.3 (Almost Arbitrarily Nesting Formula): An Almost Arbitrarily Nesting (AAN) formula is an STPL formula in which there is no time or ID variables that are used in the scope of another quantifier/freeze time operator.

For example,

$$\begin{aligned}
\varphi_1 &= x_1. \Box (\mathcal{F} - x_1 > 2 \wedge x_2. \diamond (\tau - x_2 < 0.01)) \\
\varphi_2 &= \Box \exists Id_1 @ x. \diamond (\Box \forall Id_2. (Id_1 == Id_2) \wedge (\tau - x > 2))
\end{aligned}$$

are AAN formulas. In the formula φ_1 , the time variable x_1 is not used in the scope of the x_2 . freeze time operator, and in the formula φ_2 , there is no nested quantifier/freeze time operators, therefore they are ANN STPL formulas. Whereas,

$$\begin{aligned}
\varphi_3 &= x_1. (\Box x_2. \diamond (\mathcal{F} - x_1 > 2 \wedge \tau - x_2 < 0.01)) \\
\varphi_4 &= \Box \forall Id_1 @ x_1. \Box \forall Id_2 @ x_2. \Box \forall Id_3. \\
&\quad (P(Id_3) > P(Id_1) \wedge P(Id_3) < P(Id_2))
\end{aligned}$$

are not AAN formulas. That is because in φ_3 , the variable x_1 is used in the scope of the nested variant-quantifier operator “ x_2 .”, and in φ_4 , the Id_1 is used in the scope of the second nested variant-quantifier operator “ x_2 .”.

The authors in [28] presented an efficient monitoring algorithm for TPTL formulas with arbitrary number of *independent*

time variables. Our definition of AAN formulas is adopted from their definition of *encapsulated* TPTL formulas that are TPTL formulas with only independent time variables in them. In the rest of this paper, we are only interested in AAN STPL formulas.

B. STPL Semantics

Definition 4.4 (Semantics of STPL): Consider $\mathfrak{M} = \langle \mathfrak{T}, \mathfrak{M}, \mathcal{D}, \epsilon, \zeta \rangle$ as a topological temporal model in which \mathfrak{T} is a topological space, \mathfrak{M} is a spatial valuation function, \mathcal{D} is a data-object stream, $\zeta : V_o \rightarrow \mathbb{N} \cup \{\text{NaN}\}$ is an ID-evaluating function, and $\epsilon : V_t \cup V_o \rightarrow \mathbb{N}$ is a frame-evaluating function. Here, $i \in \mathbb{N}$ is the index of current frame, $\tau : \mathbb{N} \rightarrow \mathbb{R}^+$ is a mapping function from frame numbers to their physical times, $\phi, \phi_1, \phi_2 \in STPL$ (i.e., formulas belong to the language of the grammar of STPL), V_t is a set of time variables, and V_o is a set of object ID variables. The quality value of formula ϕ with respect to \mathcal{D} at frame i with evaluations ϵ and ζ is recursively assigned as follows:

1) Semantics of Temporal Operators:

$$\begin{aligned}
[[\top]](\mathcal{D}, i, \epsilon, \zeta) &:= \top \\
[[\exists id @ x. \phi]](\mathcal{D}, i, \epsilon, \zeta) &:= \bigvee_{k \in \mathcal{OI}(\mathcal{D}(i))} ([[\phi]](\mathcal{D}, i, \epsilon[id \leftarrow k, x \leftarrow i], \zeta[id \leftarrow i])) \\
[[\tau - x \sim n]](\mathcal{D}, i, \epsilon, \zeta) &:= \begin{cases} \top & \text{if } \tau(i) - \tau(x) \sim n \\ \perp & \text{otherwise} \end{cases} \\
[[\mathcal{F} - x \sim n]](\mathcal{D}, i, \epsilon, \zeta) &:= \begin{cases} \top & \text{if } i - x \sim n \\ \perp & \text{otherwise} \end{cases} \\
[[\mathcal{F} - x \% c \sim n]](\mathcal{D}, i, \epsilon, \zeta) &:= \begin{cases} \top & \text{if } (i - x) \% c \sim n \\ \perp & \text{otherwise} \end{cases} \\
[[id_j == id_k]](\mathcal{D}, i, \epsilon, \zeta) &:= \begin{cases} \top & \text{if } \epsilon(id_j) == \epsilon(id_k) \\ \perp & \text{otherwise} \end{cases} \\
[[\neg \phi]](\mathcal{D}, i, \epsilon, \zeta) &:= \neg [[\phi]](\mathcal{D}, i, \epsilon, \zeta) \\
[[\phi_1 \vee \phi_2]](\mathcal{D}, i, \epsilon, \zeta) &:= [[\phi_1]](\mathcal{D}, i, \epsilon, \zeta) \vee [[\phi_2]](\mathcal{D}, i, \epsilon, \zeta) \\
[[\phi_1 \mathcal{U} \phi_2]](\mathcal{D}, i, \epsilon, \zeta) &:= \bigvee_{i \leq j} \left([[\phi_2]](\mathcal{D}, j, \epsilon, \zeta) \wedge \bigwedge_{i \leq k < j} [[\phi_1]](\mathcal{D}, k, \epsilon, \zeta) \right) \\
[[\bigcirc \phi]](\mathcal{D}, i, \epsilon, \zeta) &:= [[\phi]](\mathcal{D}, i + 1, \epsilon, \zeta)
\end{aligned}$$

2) Semantics of Past-Time Operators:

$$\begin{aligned}
[[\phi_1 \mathcal{S} \phi_2]](\mathcal{D}, i, \epsilon, \zeta) &:= \bigvee_{i \geq j} \left([[\phi_2]](\mathcal{D}, j, \epsilon, \zeta) \wedge \bigwedge_{j < k \leq i} [[\phi_1]](\mathcal{D}, k, \epsilon, \zeta) \right) \\
[[\odot \phi]](\mathcal{D}, i, \epsilon, \zeta) &:= [[\phi]](\mathcal{D}, i - 1, \epsilon, \zeta)
\end{aligned}$$

3) Semantics of Spatio-Temporal Operators:

$$\begin{aligned}
[[\boxplus \mathcal{T}]](\mathcal{D}, i, \epsilon, \zeta) &:= \mathfrak{M}(\boxplus \mathcal{T}, \mathcal{D}, i, \tau) \\
[[Area(\mathcal{T}) \sim r]](\mathcal{D}, i, \epsilon, \zeta) &:= \begin{cases} \perp & \text{if } f_{Area}(\mathfrak{M}(\mathcal{T}, \mathcal{D}, i, \tau)) \text{ is NaN} \\ \top & \text{if } f_{Area}(\mathfrak{M}(\mathcal{T}, \mathcal{D}, i, \tau)) \sim r \\ \perp & \text{otherwise} \end{cases}
\end{aligned}$$

$$\begin{aligned}
[[C(id) == r]](\mathcal{D}, i, \epsilon, \zeta) &:= \\
&\begin{cases} \top & \text{if } f_C(id, \mathcal{D}, i, \epsilon, \zeta) == r \\ \perp & \text{otherwise}^* \end{cases} \\
[[P(id) \sim r]](\mathcal{D}, i, \epsilon, \zeta) &:= \\
&\begin{cases} \top & \text{if } f_P(id, \mathcal{D}, i, \epsilon, \zeta) \sim r \\ \perp & \text{otherwise}^* \end{cases} \\
[[Dist(id_j, CRT_1, id_k, CRT_2) \sim r]](\mathcal{D}, i, \epsilon, \zeta) &:= \\
&\begin{cases} \top & \text{if } f_{Dist}(id_j, id_k, CRT_1, CRT_2, \mathcal{D}, i, \epsilon, \zeta) \sim r \\ \perp & \text{otherwise}^* \end{cases} \\
[[LAT(id, CRT) \sim r]](\mathcal{D}, i, \epsilon, \zeta) &:= \\
&\begin{cases} \top & \text{if } f_{LAT}(id, CRT, \mathcal{D}, i, \epsilon, \zeta) \sim r \\ \perp & \text{otherwise}^* \end{cases} \\
[[LON(id, CRT) \sim r]](\mathcal{D}, i, \epsilon, \zeta) &:= \\
&\begin{cases} \top & \text{if } f_{LON}(id, CRT, \mathcal{D}, i, \epsilon, \zeta) \sim r \\ \perp & \text{otherwise}^* \end{cases}
\end{aligned}$$

where $\sim \in \{>, <, ==, \geq, \leq\}$, and “otherwise*” has a higher priority to become true in the *if statements* if $\epsilon(id) \notin \mathcal{OI}(\mathcal{D}(i))$, and $i \leftarrow \zeta(id)$ if $\zeta(id) \neq \text{NaN}$.

In STPL, we redefine spatio-temporal valuation function \mathfrak{M} to denote $\mathfrak{M}(p, \mathcal{D}, i, \tau) := \mathcal{S}(p, k)$ where $k \leftarrow \zeta(id)$ if $\zeta(id) \neq \text{NaN}$, and $k \leftarrow i$ otherwise. Let $\Pi^{\mathcal{D}} = \{\mathcal{C}(id) \mid id \in V_o\}$ be a set of spatial variables in \mathcal{D} , $\mathbb{U}^{\mathcal{D}} = \{s \mid \forall i \in |\mathcal{D}| \forall id \in \mathcal{OI}(\mathcal{D}(i)), s = \mathcal{R}(\mathcal{D}(i), id).CS\}$, then $\mathcal{S} : \Pi^{\mathcal{D}} \times \mathbb{N} \rightarrow P(\mathbb{U}^{\mathcal{D}})$ is a mapping function that associates with every variable p and frame number i a subset of topological space i.e., $\mathcal{S}(p, i) \subseteq \mathbb{U}^{\mathcal{D}}$.

Note that we omit the semantics for some of the spatio-temporal operators in the production rule Θ except the ones stated above due to their similarity to the semantics of the presented operators.

4) *Spatio-Temporal Functions*: For the above semantics, the functions f are defined as

- $f_C(id, \mathcal{D}, i, \epsilon, \zeta)$ returns the $\mathcal{R}(\mathcal{D}(k), \epsilon(id))$.*Class* as the class of an object identified by $\epsilon(id)$ in the k 'th frame, where $k \leftarrow \zeta(id)$ if $\zeta(id) \neq \text{NaN}$, and $k \leftarrow i$ otherwise.
- $f_P(id, \mathcal{D}, i, \epsilon, \zeta)$ returns the $\mathcal{R}(\mathcal{D}(k), \epsilon(id))$.*Prob* as the probability of an object identified by $\epsilon(id)$ in the k 'th frame, where $k \leftarrow \zeta(id)$ if $\zeta(id) \neq \text{NaN}$, and $k \leftarrow i$ otherwise.
- $f_{Dist}(id_j, id_k, CRT_1, CRT_2, \mathcal{D}, i, \epsilon, \zeta)$ computes and returns the *Euclidean Distance* between the CRT_1 point of an object identified by $\epsilon(id_j)$ and CRT_2 point of an object identified by $\epsilon(id_k)$ in the k_1 'th and k_2 'th frames, respectively; and we have $k_1 \leftarrow \zeta(id_j)$ if $\zeta(id_j) \neq \text{NaN}$, and $k_1 \leftarrow i$ otherwise, and $k_2 \leftarrow \zeta(id_k)$ if $\zeta(id_k) \neq \text{NaN}$, and $k_2 \leftarrow i$ otherwise.
- $f_{LAT}(id, CRT, \mathcal{D}, i, \epsilon, \zeta)$ computes and returns the *Lateral Distance* of the CRT point of an object identified by $\epsilon(id)$ in the k 'th frame from the *Longitudinal axis*, where $k \leftarrow \zeta(id)$ if $\zeta(id) \neq \text{NaN}$, and $k \leftarrow i$ otherwise.
- $f_{LON}(id, CRT, \mathcal{D}, i, \epsilon, \zeta)$ computes and returns the *Longitudinal Distance* of the CRT point of an object identified

by $\epsilon(id)$ in the k 'th frame from the *Lateral axis*, where $k \leftarrow \zeta(id)$ if $\zeta(id) \neq \text{NaN}$, and $k \leftarrow i$ otherwise.

- $f_{Area}(\mathcal{T})$ computes and returns the area of an spatial term \mathcal{T} if $\mathcal{T} \neq \text{NaN}$, otherwise it returns NaN .

In the above functions, we use identifier variables to refer to objects in a data stream. Some parameters are point specifiers to choose a single point from all the points that belong to an object. The only function with a spatial term as an argument is the *area* function that calculates the area of a 2D bounding box. It is intuitive that for 3D reasoning, we can add the *volume* function that computes the volume of a 3D geometric shape (polyhedra in general). All the functions have \mathcal{D} , i , ϵ and ζ as fixed arguments. Functions need \mathcal{D} to access and retrieve data from, i to access to the right frame, ϵ to read the values assigned to variables, and finally, ζ to acquire the time/frame in which a variable is frozen.

Note that the above functions are application dependant, and we can add to this list based on future needs. In the next section, when we introduce an example of 3D space reasoning, we present a new spatio-temporal function.

Definition 4.5 (STPL Satisfiability): We say that the data stream \mathcal{D} satisfies the STPL formula φ under the current environment iff $[[\varphi]](\mathcal{D}, 0, \epsilon_0, \zeta_0) = \top$, which is equivalent to denote $(\mathcal{D}, 0, \epsilon_0, \zeta_0) \models \varphi$.

Note that by ϵ_0 and ζ_0 , we reset all the variables to zero. This enables the use of the presented proof system of TPTL by [28].

Example 4.1 (Evaluating a simple MTL \times S4_u formula): A sample data stream of three frames time stamped at times t_0 , t_1 , and t_2 is illustrated in Figure 3. We labeled rectangular geometric shapes in each frame by $\mathcal{C}(id_1 = 1)$ and $\mathcal{C}(id_2 = 2)$, and will refer to them by $\mathcal{C}(1)$ and $\mathcal{C}(2)$, respectively. Object $\mathcal{C}(1)$ does not change its geometric shape in all the frames, but $\mathcal{C}(2)$ evolves in each frame. The location of the $\mathcal{C}(1)$ is the same in the first two frames, but in the third frame, it moves to the bottom-right corner of the frame. The location of the $\mathcal{C}(2)$ changes constantly in each frame, that is, it first horizontally expands and moves to the bottom-left of the frame, and then expands horizontally and vertically and moves to the right-center of the frame. We are going to compute and evaluate the formula $\phi := \exists \mathcal{C}(id_1 = 1) \mathcal{U}_{[0,2]}^s \mathcal{C}(id_2 = 2)$ according to the semantics in Def. 2.6 and Def. 4.4. In Figure 4, we demonstrate the result of evaluating the subformula $\mathcal{C}(id_1 = 1) \mathcal{U}_{[0,2]}^s \mathcal{C}(id_2 = 2)$ for $i = 1$ to 3. We used \mathcal{T}_1 and \mathcal{T}_2 to refer to $\mathcal{C}(id_1 = 1)$ and $\mathcal{C}(id_2 = 2)$ in each frame, respectively. The evaluation of STPL formula ϕ starts with the following equation

$$\begin{aligned}
&[[\exists \mathcal{C}(id_1 = 1) \mathcal{U}_{[0,2]}^s \mathcal{C}(id_2 = 2)]](\mathcal{D}, 0, \epsilon_0, \zeta_0) := \\
&\mathfrak{M}(\exists \mathcal{C}(1) \mathcal{U}_{[0,2]}^s \mathcal{C}(2), \mathcal{D}, 0, \tau)
\end{aligned}$$

where, $\epsilon_0[id_1 = 1, id_2 = 2]$ and $\zeta_0[id_1 = 0, id_2 = 0]$.

The evaluating of the until subformula is computed as below

$$\mathfrak{M}(\mathcal{T}_1 \mathcal{U}_{[0,2]}^s \mathcal{T}_2, \mathcal{D}, 0, \tau) := \bigcup_{t' \in \{0,1,2\}} \left(\mathfrak{M}(\mathcal{T}_2, \mathcal{D}, t', \tau) \cap \bigcap_{0 \leq t'' < t'} \mathfrak{M}(\mathcal{T}_1, \mathcal{D}, t'', \tau) \right),$$

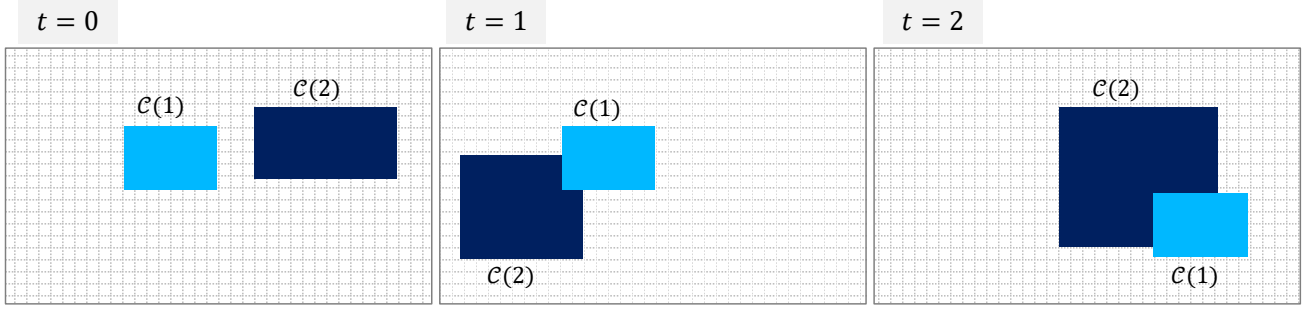


Fig. 3: An object-data stream \mathcal{D} of three frames illustrated in three time steps t_0, t_1 , and t_2 . In each frame, there are two rectangular geometric shapes denoted by identifiers 1 and 2. The lighter blue colored rectangle and the darker blue colored rectangle are identified by $\mathcal{C}(1)$ and $\mathcal{C}(2)$, respectively.

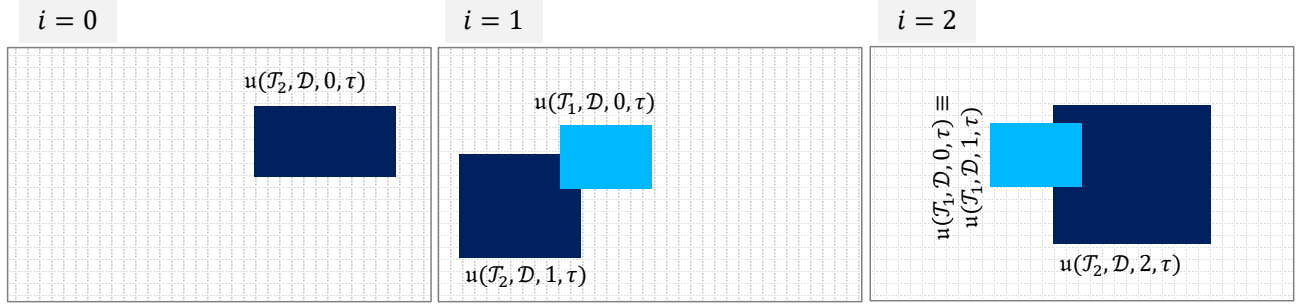


Fig. 4: The step-by-step computation of $\mathfrak{M}(\mathcal{T}_1 \mathcal{U}_{[0,2]}^s \mathcal{T}_2, \mathcal{D}, 0, \tau)$ for $i = 0$ to 2. Here, \mathcal{T}_1 and \mathcal{T}_2 refer to $\mathcal{C}(1)$ and $\mathcal{C}(2)$ in Fig. 3, respectively.

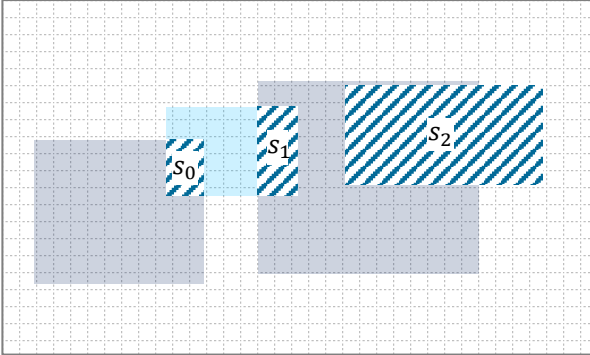


Fig. 5: $s_2 = \mathfrak{M}(\mathcal{T}_2, \mathcal{D}, 0, \tau)$, $s_0 = \mathfrak{M}(\mathcal{T}_2, \mathcal{D}, 1, \tau) \cap \mathfrak{M}(\mathcal{T}_1, \mathcal{D}, 0, \tau)$, $s_1 = \mathfrak{M}(\mathcal{T}_2, \mathcal{D}, 2, \tau) \cap \mathfrak{M}(\mathcal{T}_1, \mathcal{D}, 0, \tau) \cap \mathfrak{M}(\mathcal{T}_1, \mathcal{D}, 1, \tau)$, $\mathfrak{M}(\mathcal{T}_1 \mathcal{U}_{[0,2]}^s \mathcal{T}_2, \mathcal{D}, 0, \tau) = s_0 \cup s_1 \cup s_2$.

where $\tau(0) = 0, \tau(1) = 1$, and $\tau(2) = 2$. The above formula is equal to the below disjunctive normal formula as shown in Fig. 4

$$\begin{aligned} & \mathfrak{M}(\mathcal{C}(2), \mathcal{D}, 0, \tau) \\ & \cup \\ & (\mathfrak{M}(\mathcal{C}(2), \mathcal{D}, 1, \tau) \cap \mathfrak{M}(\mathcal{C}(1), \mathcal{D}, 0, \tau)) \\ & \cup \end{aligned}$$

$$(\mathfrak{M}(\mathcal{C}(2), \mathcal{D}, 2, \tau) \cap \mathfrak{M}(\mathcal{C}(1), \mathcal{D}, 0, \tau) \cap \mathfrak{M}(\mathcal{C}(1), \mathcal{D}, 1, \tau)).$$

The final evaluation of the above formula is depicted as hashed regions s_0, s_1 and s_2 in Fig. 5. The union of the regions is a non-empty set, hence, the spatial existential operator returns *true*.

C. MTL/STL Equivalences in STPL

Below, we represent some rewriting rules to translate time interval based formulas in MTL/STL to their equivalent STPL formulas.

$$\begin{aligned} \phi_1 \mathcal{U}_{[a,b]} \phi_2 &\equiv x. \phi_1 \mathcal{U}((a \leq \tau - x \leq b) \wedge \phi_2) \\ \phi_1 \mathcal{R}_{[a,b]} \phi_2 &\equiv x. \phi_1 \mathcal{R}((a \leq \tau - x \leq b) \implies \phi_2) \\ \Diamond_{[a,b]} \phi &\equiv x. \top \mathcal{U}((a \leq \tau - x \leq b) \wedge \phi) \\ \Diamond_{[a,b]} \phi &\equiv x. \Diamond((a \leq \tau - x \leq b) \wedge \phi) \\ \Box_{[a,b]} \phi &\equiv x. \perp \mathcal{R}((a \leq \tau - x \leq b) \implies \phi) \\ \Box_{[a,b]} \phi &\equiv x. \Box((a \leq \tau - x \leq b) \implies \phi) \end{aligned}$$

In the next section, we use specific examples of perception systems to explain each aspect of the logic individually gradually and later combined.

V. CASE STUDY

In this section, we are going to gradually demonstrate the expressivity of the STPL language using a sample object data

TABLE I: The result of applying data stream \mathcal{D} in Table II into STPL formula φ . Note that by $\llbracket \varphi \rrbracket$ we mean $\llbracket \varphi \rrbracket(\mathcal{D}, 0, \epsilon_0, \zeta_0)$. *We applied dataset “0018” from KITTI tracking benchmark for evaluating formula in Eq.(15).

φ	$\llbracket \varphi \rrbracket$	φ	$\llbracket \varphi \rrbracket$	φ	$\llbracket \varphi \rrbracket$	φ	$\llbracket \varphi \rrbracket$
Eq.(1)	\top	Eq.(2)	\perp	Eq.(3)	\perp	Eq.(4)	\perp
Eq.(5)	\perp	Eq.(8)	\top	Eq.(9)	\top	Eq.(10)	\perp
Eq.(11)	\top	Eq.(12)	\perp	Eq.(13)	\perp	Eq.(14)	\perp
Eq.(15)	\top	*Eq.(15)	\perp	Eq.(16)	\top	Eq.(17)	\top

stream corresponding to the image frames in Figure 1. There are six frames in this case-study that are taken from the KITTI² databases ([4]). We adopt a perception system based on SqueezeDet by which some desirable classes of objects in image frames are recognized. The perception classifies an object as one class from three desirable classes *Car*, *Cyclist*, and *Pedestrian*. It also assigns to each detected object a confidence level (normalized between 0 and 1), and a bounding box that surrounds the object. We also manually associate a unique object identifier to the detected objects of each frame. The data is available to the object data stream function \mathcal{D} as represented in Table II, and visualized in the frames in Fig. 1.

In the following sections, we focus on requirements that require the use of the variant-quantifiers, spatial, and spatio-temporal operators. Note that in the rest of the sections, when we translate a requirement into STPL, we will refer to the following assumptions. These assumptions enable us to write smaller formulas. They can be relaxed at the expense of more complex requirements.

Assumption 5.1: There are different perception modules to detect, track and classify the objects. That is, the object detector detects objects, and the object tracker assigns unique identifiers to the detected objects, and the classifier assigns classes to the detected objects.

Assumption 5.2: Object detector always detect objects.

Assumption 5.3: Each detected and tracked object has a unique id.

The tracker can check the detected objects through the sequence of frames but it does not imply that the classifier will assign the same class to them in all the frames.

For the requirements that are formalized into STPL in the rest of this section, we used our STPL monitoring tool to apply the data stream in Table II to each STPL formula, and presented the result in Table I.

A. Object Quantifier Examples

First, we present a requirement that enables search through a data stream to find a frame in which there are at least two unique objects from the same class.

Req. 3: There is at least one frame in which at least two unique objects are from the same class.

STPL (using all the assumptions):

$$\phi = \Diamond \exists Id_1. \exists Id_2. (Id_1 \neq Id_2 \wedge C(Id_1) = C(Id_2)). \quad (1)$$

In the above formula, the ID variable constraint requires a unique assignment of object IDs to the variables Id_1 and Id_2 . Additionally, the equivalence proposition is valid only if the classes of a unique pair of objects are equal. Also, the existential quantifier requires one assignment of objects to the ID variables that satisfy its following subformula. Lastly, the eventually operator requires one frame in which its following subformula is satisfiable.

a) Running Formula in Real Data Stream:: From the data stream \mathcal{D} in Table II, and as depicted in the frames in Fig. 1, the frame numbers 0, 2 and 3 have two pedestrians, and frame number 3 has two cars in them. Therefore, the formula is satisfiable for the given object data stream and we can denote it as $(\mathcal{D}, 0, \epsilon_0, \zeta_0) \models \phi$. Note that we can push the \Diamond operator after the existential quantifier (i.e., $\Diamond \exists Id_1. \exists Id_2. \phi \equiv \exists Id_1. \exists Id_2. \Diamond \phi$) and still expect the same result.

Next, we formalize a requirement in which we should use nested quantifiers.

Req. 4: Always, all objects in a frame must exist in the next frame.

STPL (using Assumptions 5.1-5.3):

$$\phi = \Box \forall Id_1 @x. (\bigcirc true \implies \bigcirc \exists Id_2. (Id_1 = Id_2 \wedge C(Id_1) = C(Id_2))) \quad (2)$$

The above requirement requires a fundamentally different formalization than in the formula (1). Here, we need to compare objects in any two consecutive frames which requires access to different data frames. The above formula, in part, is similar to the formula (1). Three minor differences exist: first, we have an always operator instead of the eventually operator; second, the non-equality is changed to equality; and third, the propositions are represented in the consequent of the implication. Note that the antecedent of the implication becomes always unsatisfiable for the last frame. But, the main difference lies in the use of quantifier operators. Here, we break the previous existential operator with two variables into one mixed-form universal operator that is followed by a next operator and one quantifier-formed existential operator. The reason is that the requirement expects two levels of object quantification that happen consecutively. In the first level, all the objects are considered to be assigned to the variable Id_1 . In the next level, for each object to a variable assignment that happened in the previous frame, only one quantification for the variable Id_2 that satisfies its following subformula is sufficient. All in one, the formula requires that for all the objects in a frame, there exist other objects in the next frame with the same attributes.

b) Running Formula in Real Data Stream:: Except for the frame number 4 and 5 in Table II, the rest do not satisfy the requirement that is $(\mathcal{D}, 0, \epsilon_0, \zeta_0) \not\models \phi$.

The specification formula 2 is too strict, that is, if an object existed in two consecutive frames, but disappeared in the third frame, then it violates the formula. Therefore, only if all the detected objects exist during all the frames it becomes satisfiable. We can relax this formula by adding a precondition to the antecedent of the implication. For example, we can

²<http://www.cvlibs.net/datasets/kitti/>

apply the requirement to the newly detected objects. Another simplification is possible by using the *weak next operator* \odot_w (i.e., similar to the next operator, but it does not become unsatisfiable in the last frame on a data stream where there is no next frame). Similarly, by \odot_w we denote *weak previous operator* (i.e., similar to the previous operator, but it does not become unsatisfiable in the first frame on a data stream). For more information about weak temporal operators and past LTL see the works by [54] and [55], respectively.

The below formula is a revised version of formula 2: **STPL** (using Assumptions 5.1-5.3):

$$\phi = \Box \forall Id_1 @x. \left(\left(\odot_w \forall Id_3. (Id_1! = Id_3) \right) \implies \odot_w \exists Id_2. (Id_1 == Id_2 \wedge C(Id_1) == C(Id_2)) \right) \quad (3)$$

In the above formula, the antecedent subformula checks if an object did not exist in the previous frame. Therefore, if an object existed in more than one consecutive frame, the consequent of the below formula only gets checked once for that object, and that is, for the first frame in which the object was newly detected.

c) *Running Formula in Real Data Stream::* The data stream \mathcal{D} in Table II does not satisfy the above formula which is a relaxed version of the formula in Eq. (2). That is $(\mathcal{D}, 0, \epsilon_0, \zeta_0) \not\models \phi$.

Next, we formalize a requirement in which we should use nested quantifiers and time/frame constraints in our formalization.

B. Examples with Time Constraints

Req. 5: Always, each object in a frame must exist in the next 2 frames during 1 second.

STPL (using Assumption 5.2-5.3):

$$\phi = \Box \forall Id_1 @x. \left(\left(\odot_w \forall Id_3. (Id_1! = Id_3) \right) \implies \Box \left((\tau - x \leq 1 \wedge \mathcal{F} - x \leq 2) \implies \exists Id_2. (Id_1 == Id_2 \wedge C(Id_1) == C(Id_2)) \right) \right) \quad (4)$$

Similar to the previous example, the equalities that need to hold are in the consequent of the second implication, but its antecedent is a conjunction of time and frame constraints. In this formula, there is a freeze time variable after the first quantifier operator, which is followed by an always operator. Thus, the constraints apply to the elapsed time and frames between the freeze time operator and the second always operator. Therefore, for any three consecutive frames, if the last two frames are within 1 second of the first frame, then all the objects in the first frame have to reappear in the second and third frames.

a) *Running Formula in Real Data Stream::* The same result as in the previous example holds here for the data stream \mathcal{D} in Table II that is $(\mathcal{D}, 0, \epsilon_0, \zeta_0) \not\models \phi$.

Below, we translate the requirement previously presented as in Req. 1.

Req. 6: Whenever a new object is detected, then it is assigned a class within 1 sec, after which the object does not change class until it disappears.

STPL (using Assumptions 5.1-5.3):

$$\phi = \Box \forall Id_1 @x. \left(\left(C(Id_1) == 0 \implies \varphi_{\Diamond}^{id>0} \right) \wedge \left(C(Id_1) > 0 \implies \varphi_{\Box}^{same} \right) \right) \quad (5)$$

and the predicates are defined as:

$$\varphi_{\Diamond}^{id>0} \equiv \Diamond \left((\tau - x \leq 1 \wedge \mathcal{F} - x \geq 1) \wedge \Box \exists Id_2. (Id_1 == Id_2 \wedge C(Id_2) > 0) \right)$$

$$\varphi_{\Box}^{same} \equiv \Box \forall Id_3. \left((\mathcal{F} - x \geq 1 \wedge Id_3 == Id_1) \implies C(Id_1) == C(Id_3) \right)$$

In the above formula, we evaluate the two implication-form subformulas for any objects in all the frames. If there is an object that is not classified (i.e., $C(Id_1) == 0$), then we check the consequence of the corresponding subformula. The subformula corresponding to the predicate $\varphi_{\Diamond}^{id>0}$ requires that when an unclassified object was observed, then eventually in less than a second afterward, the object always has a class being assigned to it. If there is an object that is already classified, then the second predicate has to be evaluated. The subformula equivalent to the φ_{\Box}^{same} requires that when a classified object was observed, then afterward the same object only can take the same class.

b) *Running Formula in Real Data Stream::* In the frame 1 in Table II, the object with $ID = 2$ changes its class from *cyclist* to *pedestrian*. Therefore, the data stream \mathcal{D} does not satisfy the requirement $(\mathcal{D}, 0, \epsilon_0, \zeta_0) \not\models \phi$.

C. Examples of Space and Time Requirements with 2-D Images

In the following examples, we want to demonstrate the expressivity and usability of the STPL language to capture requirements related to the detected objects and their spatial and temporal properties.

1) *Basic Spatial Examples without Quantifiers::* In the following examples, we assume that \mathcal{T} is a rectangular topological space, and it can only shift left, right, up, and down when it evolves during the time.

Example 2:

Req. 7: The intersection of a topological space \mathcal{T} with itself across all frames must not be empty.

STPL:

$$\exists \Box^s \mathcal{T} \quad (6)$$

In the following example, the topological subspaces that are the result of applying the above formula on a sequence of four frames (as shown in Fig. 6(a-d)) are depicted in Fig. 6(e). Here, the result is nonempty, hence the \exists operator evaluates to *true*.

Example 3:

TABLE II: Data stream \mathcal{D} of image frames in Fig. 1. Each row for the column headers: Frame, τ , ID, class, and Prob represent the frame number, the sampling time (e.g., here we assume that frame-per-second is 25 fps), the associated identifier to the objects, the classification confidence, respectively. Moreover, the other four headers are the data attributes (minimum and maximum lateral and longitudinal positions of coordinates of the bounding boxes) by which a bounding box is associated with each classified object. Note that some objects are not tracked correctly throughout the data stream.

Frame	τ	ID	Class	Prob	x_{min}	y_{min}	x_{max}	y_{max}
0	0	1	car	0.88	58	151	220	287
0	0	2	cyclist	0.75	479	124	690	382
0	0	3	pedestrian	0.63	522	130	632	377
0	0	4	pedestrian	0.64	861	133	954	329
1	0.04	1	car	0.88	61	152	217	283
1	0.04	2	cyclist	0.57	493	111	699	383
1	0.04	3	pedestrian	0.64	877	136	972	330
2	0.08	1	car	0.89	58	143	220	271
2	0.08	2	pedestrian	0.65	511	107	724	367
2	0.08	3	pedestrian	0.64	911	115	1001	340
3	0.12	1	car	0.92	56	139	216	266
3	0.12	2	cyclist	0.59	493	111	705	380
3	0.12	3	pedestrian	0.72	541	125	649	351
3	0.12	4	car	0.58	926	107	1004	302
3	0.12	5	pedestrian	0.76	938	118	998	332
4	0.16	1	car	0.91	53	139	217	265
4	0.16	2	pedestrian	0.80	551	126	658	356
5	0.2	1	car	0.92	52	140	216	264
5	0.2	2	cyclist	0.62	506	104	695	368
5	0.2	3	pedestrian	0.68	552	115	669	362

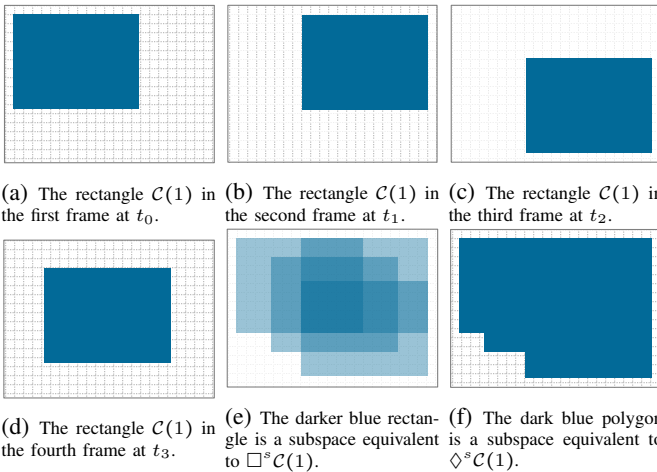
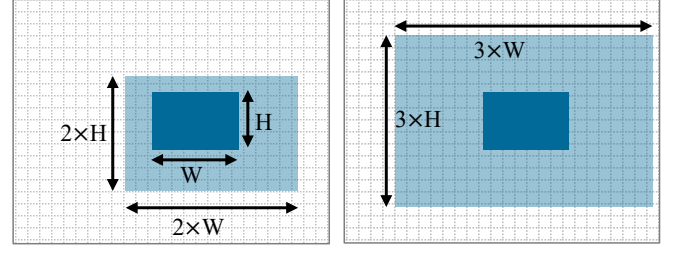


Fig. 6: The result of \square^s and \diamond^s spatial operators on a topological space over different times and frames.



(a) The smaller rectangle is \mathcal{T} and the bigger is \mathcal{T}' . (b) The smaller rectangle is \mathcal{T} and the bigger is \mathcal{T}' .

Fig. 7: (a) The bigger rectangle is a sample surrounding area for the smaller rectangle \mathcal{T} in which it can move freely and the result of formula $\square^s \mathcal{T}$ is a non-empty space. (b) For the bigger rectangle \mathcal{T}' , we have $\square^s \mathcal{T} \subseteq \mathcal{T}'$.

Req. 8: The union of a topological space \mathcal{T} with itself in all the frames has not been equal the universe.

STPL:

$$\neg \sqcup \diamond^s \mathcal{T} \quad (7)$$

In the following example, the result of applying the above formula on a sequence of four frames (as shown in Fig. 6(a-d)) is depicted in Fig. 6(f). Here, the result is not the universe; hence the $\neg \sqcup$ subformula evaluates to *true*.

Figure 7(a) demonstrates a sample occupancy space in light blue for the subspace \mathcal{T} in the darker blue. To satisfy $\square^s \mathcal{T}$, the maximum allowed movements for \mathcal{T} in lateral and longitudinal directions are $2 \times W$ and $2 \times H$, respectively. In general, the maximum subspace in which $\square^s \mathcal{T}$ is satisfiable for \mathcal{T} is a rectangle centered as \mathcal{T} with triple height and width of \mathcal{T} as shown in Fig. 7(b). The above example helps to understand the spatial evolutions that satisfies $\mathcal{T}_1 \cup^s \mathcal{T}_2$.

2) *Basic Spatial Examples with Quantifiers.*: In the following examples, the spatial requirements cannot be formalized without the use of quantifiers.

Example 4:

Req. 9: Always, all the objects must remain in the bounding box (x_1, y_1, x_2, y_2) .

STPL (using Assumption 5.2):

$$\square \forall Id. (LAT(Id, LM) \geq x_1 \wedge LAT(Id, RM) \leq x_2 \wedge LON(Id, TM) \geq y_1 \wedge LON(Id, BM) \leq y_2) \quad (8)$$

a) *Running Formula in Real Data Stream.*: The result of evaluating the above formula depends on the size and position of the bounding box. For example, if the bounding box is the same as the image frame in the data stream \mathcal{D} in Table II, then we have $(\mathcal{D}, 0, \epsilon_0, \zeta_0) \models \phi$.

Example 5:

Req. 10: Eventually, there must exist an object that at the next frame shifts to the right.

STPL (using Assumptions 5.2-5.3):

$$\diamond \exists Id_1 @x. \bigcirc \exists Id_2. (Id_1 == Id_2 \wedge LAT(Id_1, LM) < LAT(Id_2, LM)) \quad (9)$$

Note that in the above formula, the Id_1 is quantified in a freeze time quantifier to get access to the data-object values in the frozen time. If we change the first existential quantifier to the universal quantifier, then the formula represents the following requirement: “Eventually, there must exist a frame in which all the objects shift to the right in the next frame”.

b) *Running Formula in Real Data Stream*:: The data stream \mathcal{D} as in Table II satisfies the above formula $(\mathcal{D}, 0, \epsilon_0, \zeta_0) \models \phi$. For example, the pedestrian with $ID = 3$ moved to the right in the frame 1. Note that the pedestrian and the recording camera both have moved to the left, while camera’s movement was faster.

Example 6:

Req. 11: If an object shifts to the right in the next frame, then afterward, it must not shift to the right again. Alternatively, we can say, any object at most can shift to the right once.

STPL (using Assumptions 5.2-5.3):

$$\begin{aligned} & \Box \forall Id_1 @x. \left(\bigcirc_w \forall Id_2 @y. \left(\right. \right. \\ & \quad (Id_1 == Id_2 \wedge LAT(Id_1, LM) < LAT(Id_2, LM)) \implies \\ & \quad \bigcirc_w \Box \forall Id_3. (Id_2 == Id_3 \implies \\ & \quad \quad \left. LAT(Id_2, LM) \geq LAT(Id_3, LM) \right) \left. \right) \Big) \end{aligned} \quad (10)$$

Note that in the above formula, the Id_1 and Id_2 are quantified in a nesting freeze time quantifier structure, and hence, it is not an AAN formula.

c) *Running Formula in Real Data Stream*:: In Table II, the pedestrian with $ID = 3$ has moved to the right at least twice. Note that, in frame 3, the ID of the object has changed to 5. Therefore, for the data stream \mathcal{D} in Table II, we have $(\mathcal{D}, 0, \epsilon_0, \zeta_0) \not\models \phi$.

D. Examples on real-time Requirements for Perception Systems

For the examples in the rest of this section, we focus on the real-time requirements that concern detected objects in perception systems.

Example 7:

Req. 12: If a pedestrian is detected with probability higher than 0.8 in the current frame, then for the next 1 second, the probability associated with the pedestrian shouldn’t fall below 0.7, and the bounding box associated with it shouldn’t overlap with another detected bounding boxes.

STPL (using Assumptions 5.2-5.3):

$$\begin{aligned} & \Box \forall Id_1 @x. \left((C(Id_1) == Ped \wedge P(Id_1) > 0.8) \implies \right. \\ & \quad \Box (\tau - x \leq 1 \implies \\ & \quad \exists Id_2. (Id_1 == Id_2 \wedge P(Id_2) > 0.7 \wedge C(Id_2) == Ped \wedge \\ & \quad \quad \forall Id_3. (Id_2 \neq Id_3 \implies \\ & \quad \quad \quad \neg \exists (C(Id_2) \sqcap C(Id_3)))) \Big) \end{aligned} \quad (11)$$

a) *Running Formula in Real Data Stream*:: In Table II, there is no pedestrian associated with probability higher than 0.8, therefore the data stream \mathcal{D} satisfies the above formula $(\mathcal{D}, 0, \epsilon_0, \zeta_0) \models \phi$.

Example 8: The requirement below represents a situation in which all the adversarial cars in the frames from the current time forward are moving at least as fast as the ego car and in the same direction.

Req. 13: Always all the bounding boxes of the cars in the image frames do not expand.

STPL (using Assumptions 5.2-5.3):

$$\begin{aligned} & \Box \forall Id_1 @x. (C(Id_1) == Car \implies \\ & \quad \Box \forall Id_2. ((Id_1 == Id_2 \wedge C(Id_2) == Car) \implies \\ & \quad \quad Area(Id_1) \geq Area(Id_2))) \end{aligned} \quad (12)$$

In the above example, the geometric position of the objects in the space is not necessarily required, as we represented the requirement as a TQTL formula.

b) *Running Formula in Real Data Stream*:: In Table II, the bounding box of the car with $ID = 1$ has expanded in the frame 2. Therefore, the data stream \mathcal{D} does not satisfy the above formula $(\mathcal{D}, 0, \epsilon_0, \zeta_0) \not\models \phi$.

Example 9: We want to formalize a requirement specification that applies restrictions on the positions and movements of the adversarial and the ego car in all the image frames.

Req. 14: The relative position and velocity of all the cars are fixed with respect to the ego car.

STPL (using Assumptions 5.2-5.3):

$$\begin{aligned} & \Box \forall Id_1 @x. \Box \exists Id_2. \left(\bigvee (\overline{C(Id_1)} \sqcup C(Id_2)) \wedge \right. \\ & \quad \left. \bigvee (\overline{C(Id_2)} \sqcup C(Id_1)) \wedge Id_1 == Id_2 \right) \end{aligned} \quad (13)$$

Another formalization for the same requirements is as follows

$$\Box \forall Id_1. (Area(\Box^s C(Id_1)) == Area(\Diamond^s C(Id_1))) \quad (14)$$

In the above example, the geometric positions of the objects in the space are necessarily required, but again, comparing the formulas in Formula (13) with Formula (14) suggests that the second formula is more concise and readable. This example shows that having the STE operators (i.e., \Diamond^s and \Box^s) that express changes or evolutions of spacial objects in time are helpful and needed. The specification formula in Formula (14) is more readable because we use \Box^s and \Diamond^s to capture the entanglement of space and time for the same requirement while hiding some of the complexities inside the semantics of the STE operators.

c) *Running Formula in Real Data Stream*:: All of the objects in Table II have different bounding boxes in different frames. Thus, the data stream \mathcal{D} does not satisfy the above formulas $(\mathcal{D}, 0, \epsilon_0, \zeta_0) \not\models \phi$.

Example 10: In this example, we represent a sample requirement for detecting occluded objects. The example is about a high confidence OBJECT which suddenly disappears without getting close to the borders. The requirement checks if such an object existed before and next disappeared, then it has to be occluded by a previously close proximity object.



(a) The car inside the red rectangle is identified with ID 4 in frame 10, and it is annotated as “partly occluded”.



(b) The same car as in Image (a) is bounded by the yellow rectangle, and it is annotated as “largely occluded” in frame 11.



(c) The car inside the red rectangle is identified with ID 5 in frame 14, and it is annotated as “partly occluded”.



(d) The same car as in Image (c) is bounded by the yellow rectangle, and it is annotated as “largely occluded” in frame 15.



(e) The car inside the red rectangle is identified with ID 16 in frame 260, and it is annotated as “partly occluded”.



(f) The same car as in Image (e) is bounded by the yellow rectangle, and it is annotated as “largely occluded” in frame 261.

Fig. 8: We used the labels corresponding to the 390 images in the folder “0008” from the KITTI tracking benchmark. Our STPL monitoring tool detected frames 11, 15, and 261 with “largely occluded” labels as inconsistent annotations. The training data and their format are available from the links in the footnote.³

Req. 15: If there exists a high confidence OBJECT, and in the next frame, it suddenly disappears without being close to the borders, then it must be occluded by another object.

STPL (using Assumptions 5.2-5.3):

$$\Box \forall Id_1 @x. \left((\varphi_{high}^{prob} \wedge \varphi_{far}^{borders} \wedge \bigcirc \varphi_{disap}) \implies \varphi_{occ} \right) \quad (15)$$

and the predicates are defined as:

$$\begin{aligned} \varphi_{high}^{prob} &\equiv P(Id_1) > 0.8 \\ \varphi_{far}^{borders} &\equiv LON(Id_1, TM) > d_1 \wedge LON(Id_1, BM) < d_2 \\ &\quad \wedge LAT(Id_1, LM) > d_3 \wedge LAT(Id_1, RM) < d_4 \\ \varphi_{disap} &\equiv \forall Id_2. (Id_1 \neq Id_2) \\ \varphi_{occ} &\equiv \exists Id_3. \exists Id_4. \left(Id_1 \neq Id_3 \wedge Id_1 \neq Id_4 \wedge \right. \\ &\quad \left. \exists \left((C(Id_4) \sqcap C(Id_3)) \sqcup (C(Id_4) \sqcap \bigcirc^s C(Id_3)) \right) \right) \end{aligned}$$

In the above formulas, the subformula $\varphi_{far}^{borders}$ checks if the object identified by Id_1 is close to the borders of the image frame at the current time. The subformula $\forall Id_2. (Id_1 \neq Id_2)$ is to check if an object disappeared. In the subformula φ_{occ} , the Id_4 refers to the object which disappears in the next frame, and the Id_3 refers to the object that occludes the other object.

The spatial subformulas check if the bounding box of the two objects intersect each other in the current frame, or one bounding box in the current frame intersects with the other bounding box in the next frame. Similarly, we can formalize the occlusion without using STE operators by rewriting φ_{occ} as below

$$\varphi_{occ} \equiv \exists Id_3. \exists Id_4. (Id_1 \neq Id_3 \wedge Id_1 \neq Id_4 \wedge Dist(Id_4, CT, Id_3, CT) < d_5) \quad (16)$$

Note that the second formalization is less realistic because it puts a threshold on the *Euclidean distance* between two objects to infer their overlap.

d) Running Formula in Real Data Stream:: All the objects in Table II are close to the borders of the images, and the data stream does not satisfy the subformula $\varphi_{far}^{borders}$. Therefore, the data stream \mathcal{D} satisfies the the above formula $(\mathcal{D}, 0, \epsilon_0, \zeta_0) \models \phi$.

In the following, we used the above formula to partially validate the correctness of a training data stream that is used for object tracking.

e) Running Formula in Real Data Stream:: We used the formula in Eq. (15) to verify the correctness of the labeled objects as “largely occluded” in the KITTI tracking benchmark. From the 21 datasets, except for 4 of them (i.e., datasets “0013”, “0016”, “0017”, and “0018”), we detected inconsistencies in labeling objects as “largely occluded”. For

example, in the dataset “0008” (to refer to as data stream \mathcal{D}), we identified 3 frames in each a car was labeled as “*largely occluded*”, while they were inconsistent with the rest of the occluded labels. That is, we have $(\mathcal{D}, 0, \epsilon_0, \zeta_0) \neq \phi$. Our STPL monitoring tool detected the wrong labels by applying the STPL formula in Eq. (15) on the data stream in less than 2 seconds. The result of this experiment is shown in the Figure 8. We provide all the datasets as part of our monitoring tool.

Below, we translate the requirement previously presented as in Req. 2.

Req. 16: The frames per second of the camera is high enough so that for all detected cars, their bounding boxes self-overlap for at least 3 frames and for at least 10% of the area. **STPL** (using Assumptions 5.2-5.3):

$$\begin{aligned} \phi = & \Box \forall Id_1 @x. \left(\left(\odot_w \forall Id_3. (Id_1 \neq Id_3) \implies \right. \right. \\ & \Box \left((\mathcal{F} - x \geq 1 \wedge \mathcal{F} - x \leq 3) \implies \right. \\ & \quad \forall Id_2. (Id_1 == Id_2 \implies \\ & \quad \quad \text{Ratio}(\text{Area}(\mathcal{C}(Id_1) \cap \mathcal{C}(Id_2)), \\ & \quad \quad \quad \left. \text{Area}(\mathcal{C}(Id_2))) \geq 0.1) \right) \Big) \Big) \quad (17) \end{aligned}$$

In the above formula, the spatial subformula is in the form of a non-equality *ratio* function. Its first parameter represents an occupied area for the intersection of the bounding boxes of any two objects obj_1 and obj_2 referred to by Id_1 and Id_2 , respectively. The second parameter denotes the area for obj_2 . For the non-equality to be satisfiable, first, there must be a non-empty intersection between the two objects. Second, the ratio of the intersected area to the area of the second object must be at least 10%.

f) *Running Formula in Real Data Stream:* The data stream \mathcal{D} in Table II satisfies the above formula $(\mathcal{D}, 0, \epsilon_0, \zeta_0) \models \phi$.

E. Examples of Space and Time Requirements with 3D environment

1) *Missed classification scenario:* Here, we are going to show by example how 3D reasoning is possible using STPL. Specifically, we are going to show by example if the perception system misses some important objects. The six images in Figure 9 illustrates annotated information of two consecutive frames that are taken from nuScenes-lidarseg⁴ dataset ([56]). For each detected class of objects, they adopt color coding to represent the object class in the images. The color orange represents cars, and the color cyan represents drivable regions. The color-coded chart of the classes, along with their frequency in the whole dataset can be found online ([57]). In the first frame, at time t_0 , the LiDAR annotated image is shown in Fig. 9(a). The corresponding camera image for the LiDAR scene is shown in Fig. 9(c). There is a car in this image that we

pointed to in a red arrow. As one can check, there is no point cloud data associated with the identified car in the LiDAR image, and as a result, it is not detected/recognized as a car. In the next images illustrated in Fig. 9(b,d), the undetected car at t_0 is identified and annotated as a car at time t_1 . Unlike before, there are some point cloud data associated with the car by which it was detected. The semantic segmentation of the corresponding images is shown in Fig. 9(e-f). First, we will discuss how to decide if there is a missed object in the datasets, similar to what we presented here. Second, we represent a requirement specification in STPL that can formalize such missed-detection scenarios.

Example 11: For this and the next example scenarios, we have 3D coordinates of bounding volumes and 3D point clouds representing each detected object in the frames. However, the height of those points and cubes are not helpful in these cases, and therefore, we mapped them to the x - y plane by ignoring the z -axis of sensor positions (i.e., see [57]).

Let assume that the origin of the coordinate system is the center of the ego vehicle, and the y -axis is positive for all the points in front of the ego car, and the x -axis is positive for all the points to the right of the ego. That is, we have 2D bounding boxes of classified objects that are mapped to a flat ground-level environment as shown in Fig. 10. Therefore, we do not need to define new spatial functions for 3D reasoning.

Req. 17: If there is a car driving toward the ego car in the current frame, it must exist in the previous frame.

STPL (using Assumptions 5.2-5.3):

$$\Box \forall Id_1. \forall Id_3 @x. \left((\varphi_{exist}^{car} \wedge \varphi_{close}^{dist}) \implies \odot_w \varphi_{existed}^{before} \right) \quad (18)$$

and the predicates are defined as:

$$\varphi_{exist}^{car} \equiv (C(Id_1) == Car) \wedge (C(Id_3) == Drv)$$

$$\varphi_{close}^{dist} \equiv LON(Id_1, BM) \leq 1.2 \times LON(Id_3, BM) \wedge$$

$$LON(Id_1, TM) \geq 0.5 \times LON(Id_3, BM) \wedge$$

$$LAT(Id_1, CT) \geq LAT(Id_3, LM) \wedge$$

$$LAT(Id_1, CT) \leq LAT(Id_3, RM)$$

$$\varphi_{existed}^{before} \equiv \exists Id_2. (C(Id_2) == Car \wedge Id_1 == Id_2 \wedge$$

$$Dist(Id_2, CT, \mathbb{U}, CT) > Dist(Id_1, CT, \mathbb{U}, CT))$$

Note that in the above 2D spatial functions, we used BM and TM in contrast to their original semantics in the previous examples due to the change of origin of the universe. Also, we assume that the perception system uses an accurate object tracker that assigns unique IDs to objects during consecutive frames. We used Id_1 , Id_2 , and Id_3 to refer to a car in the current frame, a car in the previous frame, and the drivable region. Note that we needed to use the previous frame operator to check if an existing car was absent in the previous frame. That is, in $\varphi_{existed}^{before}$, we check if the car identified by Id_2 matches with the same car in the previous frame. The antecedent of the formula as in Eq. (18) holds in the current

³Training data: http://www.cvlibs.net/datasets/kitti/eval_tracking.php, and data format: <https://github.com/JonathonLuiten/TrackEval/blob/master/docs/KITTI-format.txt>

⁴<https://www.nuscenes.org/nuscenes?sceneId=scene-0274&frame=0&view=lidar>

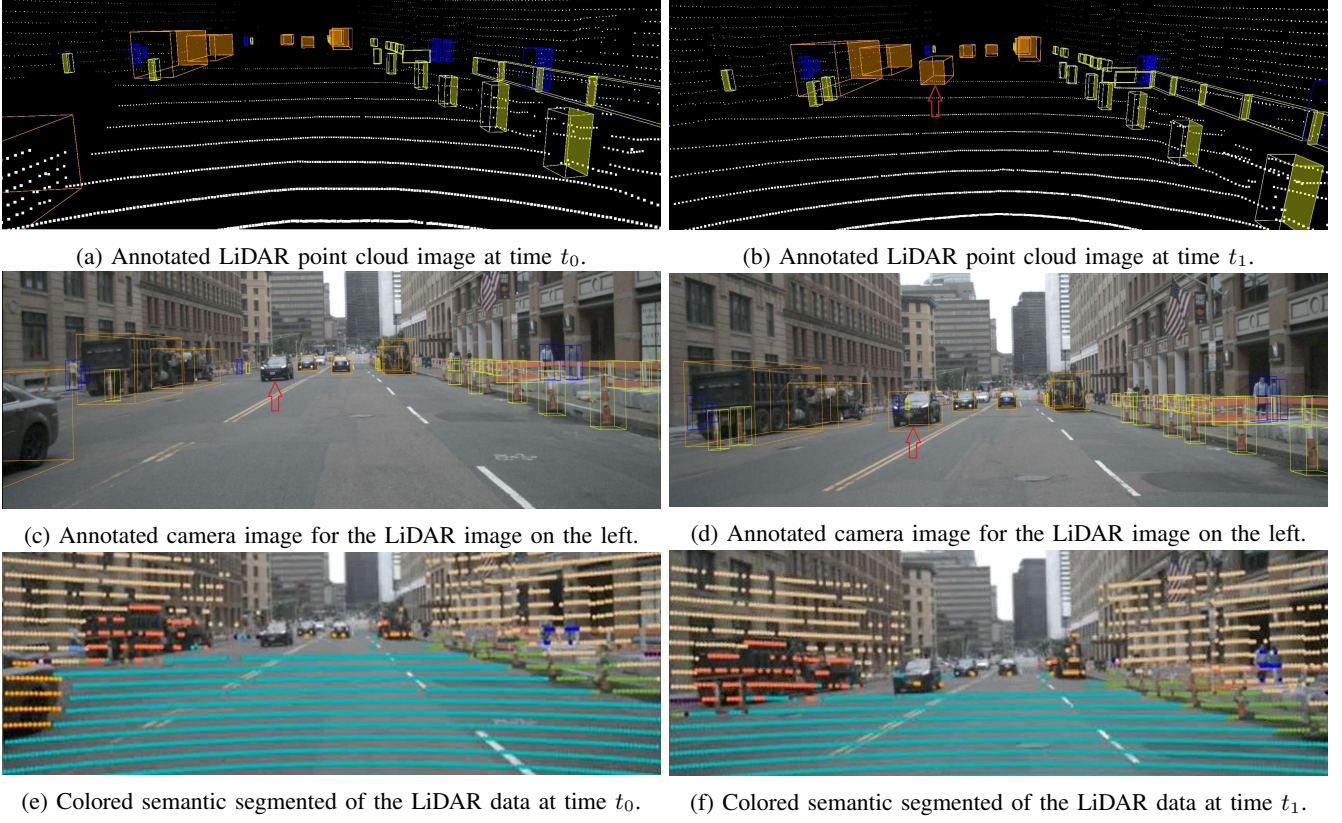


Fig. 9: Two LiDAR and Camera frames annotated data along with the semantic segmentation data are taken from NuScenes LidarSeg dataset (Scene-0247) ([56]).

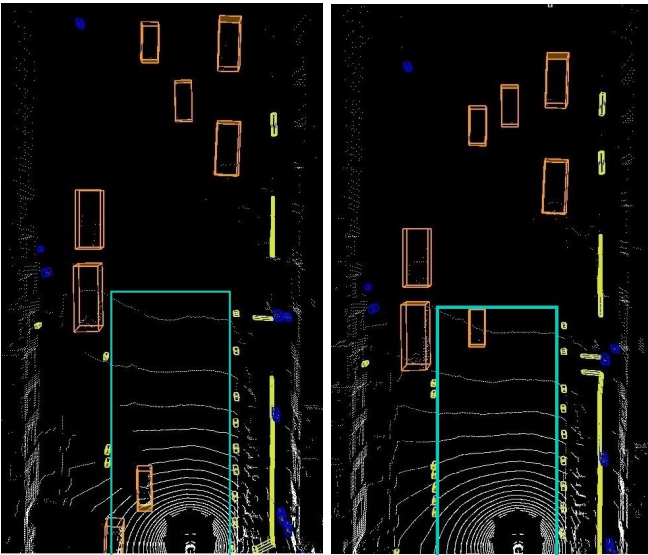


Fig. 10: The bird-view of LiDAR point clouds for the two consecutive frames in Fig. 9 where the drivable area in front of the ego is shown.

frame, but the consequent of it fails because the car that exists in the current frame did not exist in the previous frame. Thus, the data stream shown as image frames in Fig. 10 falsifies the formula.

It is more realistic to formulate the same requirement using lane-based coordinate systems, if the perception system detects different lanes. Consequently, we can simplify the subformula φ_{close}^{dist} to encode if the cars drive in the same lane.

2) *3D occlusion scenario*: In Figure 11, there are four frames captured at t_0 to t_3 . In the second and third frames, an occluded car (pointed to a red arrow) is detected. The perception system detected a car for which there is no information from the sensors (the cubes in frames 2 and 3 are empty, and the cameras cannot see the occluded vehicle). Although this can be the desired behavior for a perception system that does object tracking, here we are going to formalize a requirement that detects similar cases as wrong classifications.

For this example, we need to define a new 3D spatial function *Visible* by which we can check if given two cars are visible from the view of a third car. Additionally, we need to add a data attribute *Empty* to the data-object stream \mathcal{D} that determines if a bounding volume of an object is empty (e.g., $\mathcal{R}(\mathcal{D}(i), ID).PC == \emptyset$ checks if there is no point could associate with object identified by ID) or not. For instance, by $\mathcal{R}(\mathcal{D}(i), ID).Empty$ we check if an object identified by ID in the i 'th frame is empty. We use function $E(id)$ as a new syntax that serves as above.

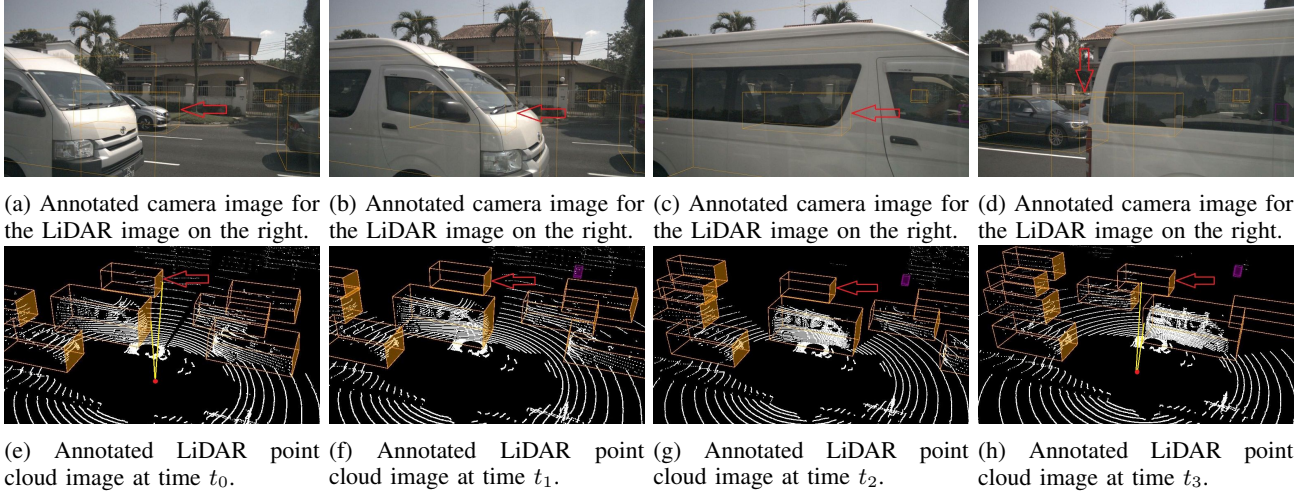


Fig. 11: Two LiDAR and Camera frames annotated data are taken from NuScenes LidarSeg dataset (Scene-0399) ([56]). The images are taken by the back-left camera as represented in sensor-position image available at nuScenes website ([57]).

$$[[V(id, CRT, id, id) \sim r]](\mathcal{D}, i, \epsilon, \zeta) := \begin{cases} \top & \text{if } f_{visible}(id, CRT, id, id, \mathcal{D}, i, \epsilon, \zeta) \sim r \\ \perp & \text{otherwise}^* \end{cases}$$

$f_{visible}(id_1, CRT, id_2, id_3, \mathcal{D}, i, \epsilon, \zeta)$ returns *true* if the objects identified by $\epsilon(id_2)$ and $\epsilon(id_3)$ are visible from the view point CRT of $\epsilon(id_1)$ in the k 'th frame, where $k \leftarrow \zeta(id)$ if $\zeta(id) \neq \text{NaN}$, and $k \leftarrow i$ otherwise. If one or both are invisible from the view point of object $\epsilon(id_1)$, then the function returns *false*.

Example 12:

Req. 18: Any detected car (using the LiDAR data) driving the same direction on the left side of the ego car must include some point cloud data in its bounding volume unless it is occluded.

STPL (using Assumptions 5.1-5.3):

$$\begin{aligned} & \Box \forall Id_1. \forall Id_2. \left(\left(\neg E(Id_1) \wedge \neg E(Id_2) \wedge (Id_1 \neq Id_2) \right. \right. \\ & \quad \wedge (C(Id_1) == Car) \wedge (C(Id_2) == Car) \\ & \quad \wedge LAT(Id_1, RM) < -1 \wedge LAT(Id_2, RM) < -1 \\ & \quad \wedge LAT(Id_1, RM) > -6 \wedge LAT(Id_2, RM) > -6 \\ & \quad \wedge MD(Id_1) == MD(Id_2) \\ & \quad \wedge V(\mathbb{U}, CT, Id_1, Id_2) \\ & \quad \left. \wedge \neg V(\mathbb{U}, CT, Id_1, Id_2) \right) \implies \\ & \quad \bigcirc \left(V(\mathbb{U}, CT, Id_1, Id_2) \right. \\ & \quad \quad \mathcal{R} \\ & \quad \quad \left. \left. (E(Id_1) \wedge \neg E(Id_2)) \right) \right) \end{aligned} \quad (19)$$

In the above formula, we keep track of two cars using Id_1 and Id_2 that are to the left of the ego car (their distance has to be limited between 1 to 6 meters from the left side of

the ego car). We assume that the perception system returns the moving direction of each classified object, and we use function MD to retrieve the direction for a given object identifier. Note that this function can be replaced by a spatial formula that uses the coordinates of an object in different frames to calculate its moving direction. The subformula $V(\mathbb{U}, CT, Id_1, Id_2)$ requires a visible angle between the two cars from the point of view of the ego car (i.e., the center point of the \mathbb{U}) to return true. We draw a sample visible angle in the first and fourth frames in yellow. For the two cars that we could find a visible angle for them in the first frame, there is none in frames 2 and 3. Additionally, there is no point cloud in the occluded car's bounding volume in frames 2 and 3. That satisfies the whole formula until the implies operator. The consequence of the implication is a release formula to be satisfiable from the next time/frame. In the release formula, the right-hand side requires the occluded object to be empty, and only when it becomes visible again, it can be non-empty. The whole formula is satisfiable for the pair of cars we discussed here. The data stream shown as image frames in Fig. 11 satisfies the formula in Eq. (19).

VI. EXPERIMENTS AND RESULTS

A. Correctness and Complexity Analysis

Let $\hat{\rho}$ be an input signal of size $|\hat{\rho}|$, φ be an AAN STPL formula of size $|\varphi|$ (note that size of a formula is the summation of the number of spatial, temporal and spatio-temporal subformulas), $|V_t|$ be the size of freeze time variables (or 1 if there is none), S_{id} be the maximum number of used ID variables in the scope of a quantifier operator, and S_{obj} be the maximum number of objects in a single frame in $\hat{\rho}$. If φ is a TPTL formula, then it is known from [28] that the upper bound time complexity for the variable-bounded TPTL monitoring algorithm is $O(|V_t| \times |\varphi| \times |\hat{\rho}|^2)$, which is polynomial. Additionally, the upper bound space complexity of the presented algorithm by [28] is $O(|\varphi| \times |\hat{\rho}|)$. Our STPL monitoring algorithm is founded based on the TPTL

TABLE III: Statistics on execution-time for different formulas and data stream sizes. We used the Berkely DeepDrive (BDD) dataset to compute the results. *m-time* and *e-time* represent the required time (in second) for releasing memories and executing the monitoring algorithm, respectively.

$ \hat{\rho} $	$ \varphi_t $	$ \varphi_s $	$ V_t $	S_{obj}	S_{id}	m-time	e-time
<i>quantifier-formed STPL Formula (8) without spatial operators</i>							
25	9	0	0	20	1	0	0.002
50	9	0	0	20	1	0	0.001
100	9	0	0	23	1	0	0.005
200	9	0	0	24	1	0	0.008
<i>mix-formed STPL Formula (9) without spatial operators</i>							
25	7	0	1	20	2	0	0.132
50	7	0	1	20	2	0	0.519
100	7	0	1	23	2	0	2.76
200	7	0	1	24	2	0	11.31
<i>mix-formed STPL Formula (13) with SPE operators</i>							
25	9	8	1	20	2	0.004	1.25
50	9	8	1	20	2	0.003	4.13
100	9	8	1	23	2	0.005	16.32
200	9	8	1	24	2	0.005	63.52
<i>quantifier-formed STPL Formula (14) with STE operators</i>							
25	3	4	0	20	1	0	0.006
50	3	4	0	20	1	0	0.029
100	3	4	0	23	1	0	0.119
200	3	4	0	24	1	0	0.176
<i>mix-formed STPL Formula (15) with spatial terms</i>							
25	29	9	1	20	3	0.023	2.23
50	29	9	1	20	3	0.023	4.97
100	29	9	1	23	3	0.037	16.07
200	29	9	1	24	3	0.043	46.88
<i>mix-formed STPL Formula (16) without spatial terms</i>							
25	29	0	1	20	3	0	1.16
50	29	0	1	20	3	0	2.73
100	29	0	1	23	3	0	10.41
200	29	0	1	24	3	0	33.69

monitoring algorithm, but there are two major additions to the TPTL syntax and semantics. First, in the STPL grammar represented in Def. 4.1, the freeze time operator follows existential/universal quantifiers to quantify ID variables that are used in the production rule Θ . We call this extension of the TPTL language the Quantifiable TPTL (QTPTL). Next is the production rule \mathcal{T} that produces purely spatio-temporal formulas (Π and Ξ \mathcal{T} quantify the spatio-temporal in a constant time). The last addition to the QTPTL results in the STPL language. Therefore, we only analyze time and space complexity of our algorithm for parts that concern the two aforementioned additions.

Our proposed monitoring algorithm is based on the Dynamic Programming (DP) algorithm by [28] and, therefore, to consider the first addition, we need to evaluate each ID variable related subformula at most $(S_{obj})^{S_{id}}$ times. This also requires extra space to build the DP tables. Therefore, the upper bound time and space complexity of the QTPTL algorithms increases

to $O((S_{obj})^{S_{id}} \times |V_t| \times |\varphi| \times |\hat{\rho}|^2)$ and $O((S_{obj})^{S_{id}} \times |\varphi| \times |\hat{\rho}|)$, respectively.

Finally, we consider spatial and spatio-temporal subformulas denoted as φ_s in addition to temporal ones denoted as φ_t to do complexity analysis of the STPL algorithm. It is easy to see that the production rule \mathcal{T} has the same grammar as MTL/STL, except that the logical operators are replaced with spatial ones. Therefore, the time/space complexity of monitoring these formulas follows the same complexity as in MTL/STL monitoring algorithms except for the spatial operations. In MTL/STL, all the logical operations compute in constant time. However, for spatial operations, depending on the used data structure for representing the spatial terms, this might not hold. In [Appendix VI](#).

Appendix: Complexity Analysis, we calculate exponential lower bound for some spatio-temporal formulas where the linked-list was used to represent the spatial terms. That is, if we do not exploit the geometrical properties of the spatial terms while storing them, then we get an exponential complexity for the spatial operations. Whereas, if we use some geometry-sensitive data structures such as *region Quadrees* and *region Octrees* for storing and computing 2D and 3D spatial terms (e.g., see [58], [59]), respectively, then, we get a polynomial time and space complexity, e.g., [60]. Assume that we can decompose our d -dimensional topological space into $2^{n \times d}$ cells, where 2^n is the constant resolution along each axis. Construction of an image Quadtree/Octree is linear in the size of the image. For example, for a binary image with resolution of 2^{2n} , it is $K = O(2^{2n})$. The union and intersection algorithm for Quadrees, in the worst case requires to visit all the nodes in the trees, which can be done in K times. For computing a spatio-temporal formula φ_s , at each time-step, in the worst case, it requires as many spatial operations as linear to the size of the formula. Therefore, the time complexity of computing the formula φ_s against an input signal $\hat{\rho}$ is as follows:

- $O(|\hat{\rho}| \times |\varphi_s| \times K)$, if there is no time/frame intervals in the formula and no frozen id variable is used in the formula. Note that K is a big constant (i.e., K is a function of the dimension and the resolution of the space) and we did not omit it to emphasize its impact on the computation.
- $O(|\hat{\rho}| \times |\varphi_s| \times K \times c)$, if there are time/frame intervals in the formula and no frozen id variable is used in the formula, where c is as defined by [61].
- $O(|\hat{\rho}| \times |\varphi_s| \times K \times |V_t|)$, if there is no time/frame intervals in the formula, but there are frozen ID variables used in the formula.
- $O(|\hat{\rho}| \times |\varphi_s| \times K \times c \times |V_t|)$, if there are time/frame intervals in the formula, and there are frozen ID variables used in the formula.

Overall, the upper bound time and space complexity of the STPL algorithm are $O((S_{obj})^{S_{id}} \times |V_t| \times |\varphi| \times |\hat{\rho}|^2 \times K \times c)$ and $O((S_{obj})^{S_{id}} \times |\varphi| \times |\hat{\rho}| \times K)$, respectively.

In our implementation of the monitoring algorithms (discussed in [Appendix VI](#).

Appendix: Monitoring Algorithm), we focus on the future fragment of the STPL logic to avoid complexity (e.g, by

excluding past-time operators as presented in [Appendix VI. Appendix: STPL Future Syntax](#)). That is, we improved the space complexity of STPL formulas without spatial terms by decoupling the DP tables into two separate tables: one dedicated to the values of subformulas at the current time step, and the other for their frozen values along the time horizon. Therefore, we reduced the space complexity to $O((S_{obj})^{S_{id}} \times (|\varphi_t| + |\hat{\rho}|))$ for non-spatial STPL formulas and spatial formulas without time/frame intervals in them. For improving the exponential complexity of the spatial STPL formulas, we merge the fragmented subsets after spatial operations. Additionally, if there is no frozen ID variable used in a spatial formula, we only evaluate it once. Some optimizations can be done based on the content of the formulas, for example, if a temporal formula does not have *globally*, *eventually*, *until* and *release* operators in it, then we deduce the needed horizon length of the input signal accordingly (i.e., next time operator only requires the evaluation of the first two frames). Also, we interpret the time/frame constraints in a formula to possibly ignore the evaluation of the affected subformulas accordingly.

The correctness of the algorithm with respect to the presented syntax and semantics of STPL can be proven by using the correctness proofs that are presented for the TPTL and MTL monitoring algorithms by [28] and [61].

We have released an executable version of the code for both Linux and Windows OS in a public repository in GitLab [30]. Our tool can be run in standalone mode or as part of Matlab. Additionally, there are data stream files and input configuration files that cover most of the examples in the previous sections, as well as the sensitivity analysis result in the following section.

B. Sensitivity Analysis

We hand-selected some of the presented example formulas to cover different possible combinations for the operators and quantifiers, and to demonstrate how the computing time scales concerning the size of a data stream and the formulas. For this experiment, we used the DeepDrive dataset⁵ ([62]). As indicated in the last column of Table III, the performance of the STPL monitoring algorithm for hundreds of monitoring frames (including thousands of objects) is still feasible for online and offline monitoring.

Remark 6.1: For online monitoring, we will add past-time operators and redesign the algorithm for parallel computing. Our experiments suggest that online monitoring using the sliding window method (for the time horizon of seconds) is feasible. That is, given the execution time for monitoring an STPL formula over a given horizon, we can estimate the maximum size of the sliding window for online monitoring of that formula.

Some statistics about the experiments are summarized in Table III. In these experiments, we used a Windows 10 machine with Intel Core i7 CPU 8550U @ 1.8GHZ, 16GB RAM, and Matlab R2020a. The algorithm is implemented in C language and compiled to be used in Matlab.

VII. CONCLUSIONS

In this paper, we presented Spatio-Temporal Quality Logic (STPL), which is a logic that can be used for reasoning over data streams of perception systems. STPL merges and extends other practical logics such as STL [17], TPTL [19], and $S4_u$ [20] with new functions and relational operations that enable topological reasoning. STPL also comes with publicly available monitoring tools [30] which can be used for offline perception system analysis, or even for retrieval of scenarios from databases with perception data streams for further system testing [16].

Currently, we are investigating online monitoring algorithms [63], and Domain Specific Languages (DSL) for better usability and maintenance [64]. In the future, we will improve the performance of our tools through parallelization. It would also be interesting to see if meaningful robustness semantics [45] could be defined in order to support test case generation or even self-supervised training of neural networks. Lastly, we will look into perception requirements under different environment conditions, e.g., rain [65], fog/snow [66], etc.

ACKNOWLEDGMENT

This work was partially supported by NSF under grants CNS-2039087, CNS-2038666, IIP-1361926 and the NSF I/UCRC Center for Embedded Systems.

REFERENCES

- [1] W. Schwarting, J. Alonso-Mora, and D. Rus, "Planning and decision-making for autonomous vehicles," *Annual Review of Control, Robotics, and Autonomous Systems*, vol. 1, pp. 187–210, 2018.
- [2] T. B. Lee, "Report: Software bug led to death in uber's self-driving crash," *Ars Technica*, vol. May 07, 2018.
- [3] B. Templeton, "Tesla in taiwan crashes directly into overturned truck, ignores pedestrian, with autopilot on," *Forbes*, vol. June 2, 2020.
- [4] A. Geiger, P. Lenz, C. Stiller, and R. Urtasun, "Vision meets robotics: The kitti dataset," *The International Journal of Robotics Research*, vol. 32, no. 11, pp. 1231–1237, 2013.
- [5] B. Wu, F. Iandola, P. H. Jin, and K. Keutzer, "Squeezedet: Unified, small, low power fully convolutional neural networks for real-time object detection for autonomous driving," in *Proceedings of the IEEE Conference on Computer Vision and Pattern Recognition Workshops*, 2017, pp. 129–137.
- [6] E. Yurtsever, J. Lambert, A. Carballo, and K. Takeda, "A survey of autonomous driving: Common practices and emerging technologies," *IEEE Access*, vol. 8, pp. 58 443–58 469, 2020.
- [7] S. R. Richter, Z. Hayder, and V. Koltun, "Playing for benchmarks," in *IEEE International Conference on Computer Vision, ICCV*, 2017, pp. 2232–2241.
- [8] H. Abbas, M. E. O'Kelly, A. Rodionova, and R. Mangharam, "A driver's license test for driverless vehicles," *Mechanical Engineering*, vol. 139, pp. S13–S16, 2017.
- [9] M. Hekmatnejad, S. Yaghoubi, A. Dokhanchi, H. B. Amor, A. Shrivastava, L. Karam, and G. Fainekos, "Encoding and monitoring responsibility sensitive safety rules for automated vehicles in signal temporal logic," in *17th ACM-IEEE International Conference on Formal Methods and Models for System Design (MEMOCODE)*, 2019.
- [10] C. E. Tuncali, G. Fainekos, D. Prokhorov, H. Ito, and J. Kapinski, "Requirements-driven test generation for autonomous vehicles with machine learning components," *IEEE Transactions on Intelligent Vehicles*, vol. 5, pp. 265–280, 2020.
- [11] T. Dreossi, D. J. Fremont, S. Ghosh, E. Kim, H. Ravanbakhsh, M. Vazquez-Chanlatte, and S. A. Seshia, "Verifai: A toolkit for the formal design and analysis of artificial intelligence-based systems," in *International Conference on Computer Aided Verification*. Springer, 2019, pp. 432–442.

⁵<https://bdd-data.berkeley.edu/>

- [12] T. Dreossi, A. Donzé, and S. A. Seshia, “Compositional falsification of cyber-physical systems with machine learning components,” *Journal of Automated Reasoning*, vol. 63, pp. 1031–1053, 2019.
- [13] A. Corso, R. J. Moss, M. Koren, R. Lee, and M. J. Kochenderfer, “A survey of algorithms for black-box safety validation,” *arXiv preprint arXiv:2005.02979*, 2020.
- [14] T. Dreossi, D. J. Fremont, S. Ghosh, E. Kim, H. Ravanbakhsh, M. Vazquez-Chanlatte, and S. A. Seshia, “VerifAI: A toolkit for the formal design and analysis of artificial intelligence-based systems,” in *31st International Conference on Computer Aided Verification (CAV)*, Jul. 2019.
- [15] J. DeCastro, K. Leung, N. Aréchiga, and M. Pavone, “Interpretable policies from formally-specified temporal properties,” in *2020 IEEE 23rd International Conference on Intelligent Transportation Systems Conference (ITSC)*, Sep. 2020.
- [16] S. K. Bshetty, H. B. Amor, and G. Fainekos, “DeepCrashTest: turning dashcam videos into virtual crash tests for automated driving systems,” in *International Conference on Robotics and Automation (ICRA)*, 2020.
- [17] O. Maler and D. Nickovic, “Monitoring temporal properties of continuous signals,” in *Proceedings of FORMATS-FTRTFT*, ser. LNCS, vol. 3253, 2004, pp. 152–166.
- [18] A. Dokhanchi, H. B. Amor, J. V. Deshmukh, and G. Fainekos, “Evaluating perception systems for autonomous vehicles using quality temporal logic,” in *International Conference on Runtime Verification*. Springer, 2018, pp. 409–416.
- [19] R. Alur and T. A. Henzinger, “A really temporal logic,” *J. ACM*, vol. 41, pp. 181–203, 1994.
- [20] M. Aiello, I. E. Pratt-Hartmann, and J. F. van Benthem, “Handbook of spatial logics.” Springer, 2007.
- [21] Z. Manna and A. Pnueli, *The Temporal Logic of Reactive and Concurrent Systems — Specification*. Springer, 1992.
- [22] D. Gabelaia, R. Kontchakov, A. Kurucz, F. Wolter, and M. Zakharyashev, “Combining spatial and temporal logics: expressiveness vs. complexity,” *Journal of artificial intelligence research*, vol. 23, pp. 167–243, 2005.
- [23] T. Li, “Spatio-temporal specification language for cyber-physical systems,” in *International Conference on Formal Engineering Methods*. Springer, 2019, pp. 517–521.
- [24] H. Sun, M. H. Ang, and D. Rus, “A convolutional network for joint deraining and dehazing from a single image for autonomous driving in rain,” in *2019 IEEE/RSJ International Conference on Intelligent Robots and Systems (IROS)*. IEEE, 2019, pp. 962–969.
- [25] J. Campbell, H. B. Amor, M. H. Ang, and G. Fainekos, “Traffic light status detection using movement patterns of vehicles,” in *2016 IEEE 19th International Conference on Intelligent Transportation Systems (ITSC)*. IEEE, 2016, pp. 283–288.
- [26] B. Qin, Z. J. Chong, S. H. Soh, T. Bandyopadhyay, M. H. Ang, E. Frazzoli, and D. Rus, “A spatial-temporal approach for moving object recognition with 2d lidar,” in *Experimental Robotics*. Springer, 2016, pp. 807–820.
- [27] N. Markey and J.-F. Raskin, “Model checking restricted sets of timed paths,” *Theoretical Computer Science*, vol. 358, pp. 273–292, 2006.
- [28] A. Dokhanchi, B. Hoxha, C. E. Tuncali, and G. Fainekos, “An efficient algorithm for monitoring practical tptl specifications,” in *2016 ACM/IEEE International Conference on Formal Methods and Models for System Design (MEMOCODE)*. IEEE, 2016, pp. 184–193.
- [29] A. Elgyut, T. Ferrere, and T. A. Henzinger, “Monitoring temporal logic with clock variables,” in *Formal Modeling and Analysis of Timed Systems (FORMATS)*, ser. LNCS, vol. 11022. Springer, 2018.
- [30] Spatio-Temporal Perception Logic (STPL) Offline Monitoring Tools, “<https://gitlab.com/vnv-tools/STPL>.”
- [31] K. He, M. Lahijanian, L. E. Kavraki, and M. Y. Vardi, “Automated abstraction of manipulation planning for cost-based reactive synthesis,” *IEEE Robotics and Automation Letters*, vol. 4, no. 2, pp. 285–292, 2018.
- [32] —, “Towards manipulation planning with temporal logic specifications,” in *2015 IEEE international conference on robotics and automation (ICRA)*. IEEE, 2015, pp. 346–352.
- [33] H. W. Guesgen, “Spatial reasoning based on allen’s temporal logic,” International Computer Science Institute, Tech. Rep. TR-89-049, 1989.
- [34] A. G. Cohn, B. Bennett, J. Gooday, and N. M. Gotts, “Qualitative spatial representation and reasoning with the region connection calculus,” *GeoInformatica*, vol. 1, no. 3, pp. 275–316, 1997.
- [35] E. Bartocci, F. Corradini, M. R. D. Berardini, E. Merelli, and L. Tesei, “Shape calculus. a spatial mobile calculus for 3d shapes,” *Scientific Annals of Computer Science*, vol. 20, pp. 1–31, 2010.
- [36] M. Bhatt and S. Loke, “Modelling dynamic spatial systems in the situation calculus,” *Spatial Cognition & Computation*, vol. 8, pp. 86–130, 2008.
- [37] F. Dylla, J. H. Lee, T. Mossakowski, T. Schneider, A. V. Delden, J. V. D. Ven, and D. Wolter, “A survey of qualitative spatial and temporal calculi: Algebraic and computational properties,” *ACM Computing Surveys*, vol. 50, 2017.
- [38] H. Kress-Gazit and G. J. Pappas, “Automatic synthesis of robot controllers for tasks with locative prepositions,” in *IEEE International Conference on Robotics and Automation (ICRA)*, May 2010, pp. 3215–3220.
- [39] D. Summers-Stay, T. Cassidy, and C. Voss, “Joint navigation in commander/robot teams: Dialog & task performance when vision is bandwidth-limited,” in *Third Workshop on Vision and Language*, 2014.
- [40] S. Linker and M. Hilscher, “Proof theory of a multi-lane spatial logic,” in *International Conference on Theoretical Aspects of Computing (ICTAC)*, ser. LNCS, vol. 8049. Springer, 2013, pp. 231–248.
- [41] S. M. Loos, A. Platzer, and L. Nistor, “Adaptive cruise control: Hybrid, distributed, and now formally verified,” in *Formal Methods*, ser. LNCS, vol. 6664. Springer, 2011, pp. 42–56.
- [42] I. Haghghi, A. Jones, Z. Kong, E. Bartocci, R. Grosu, and C. Belta, “Spatel: a novel spatial-temporal logic and its applications to networked systems,” in *Proceedings of the 18th International Conference on Hybrid Systems: Computation and Control*, 2015, pp. 189–198.
- [43] L. Nenzi, L. Bortolussi, V. Ciancia, M. Loret, and M. Massink, “Qualitative and quantitative monitoring of spatio-temporal properties,” in *Runtime Verification*. Springer, 2015, pp. 21–37.
- [44] M. Ma, E. Bartocci, E. Lifland, J. Stankovic, and L. Feng, “SaSTL: Spatial aggregation signal temporal logic for runtime monitoring in smart cities,” in *ACM/IEEE 11th International Conference on Cyber-Physical Systems (ICCPs)*, 2020, pp. 51–62.
- [45] E. Bartocci, J. Deshmukh, A. Donzé, G. Fainekos, O. Maler, D. Nickovic, and S. Sankaranarayanan, “Specification-based monitoring of cyber-physical systems: A survey on theory, tools and applications,” in *Lectures on Runtime Verification - Introductory and Advanced Topics*, ser. LNCS. Springer, 2018, vol. 10457, pp. 128–168.
- [46] F. B. Buonamici, G. Belmonte, V. Ciancia, D. Latella, and M. Massink, “Spatial logics and model checking for medical imaging,” *International Journal on Software Tools for Technology Transfer*, pp. 1–23, 2019.
- [47] Z. Liu, M. Jiang, and H. Lin, “A graph-based spatial temporal logic for knowledge representation and automated reasoning in cognitive robots,” *arXiv preprint arXiv:2001.07205*, 2020.
- [48] E. A. Gol, E. Bartocci, and C. Belta, “A formal methods approach to pattern synthesis in reaction diffusion systems,” in *53rd IEEE Conference on Decision and Control*. IEEE, 2014, pp. 108–113.
- [49] M. Huth and M. Ryan, *Logic in Computer Science: Modelling and reasoning about systems*. Cambridge university press, 2004.
- [50] D. J. Fremont, X. Yue, T. Dreossi, S. Ghosh, A. L. Sangiovanni-Vincentelli, and S. A. Seshia, “Scenic: Language-based scene generation,” *arXiv:1809.09310*, Tech. Rep., 2018.
- [51] R. Kontchakov, A. Kurucz, F. Wolter, and M. Zakharyashev, “Handbook of spatial logics: Spatial logic + temporal logic = ?” Springer, 2007, pp. 497–564.
- [52] R. Koymans, “Specifying real-time properties with metric temporal logic,” *Real-Time Systems*, vol. 2, no. 4, pp. 255–299, 1990.
- [53] D. Gordon, A. Farhadi, and D. Fox, “Re³: Real-time recurrent regression networks for visual tracking of generic objects,” *IEEE Robotics and Automation Letters*, vol. 3, no. 2, pp. 788–795, 2018.
- [54] C. Eisner and D. Fisman, “Weak vs. strong temporal operators,” *A Practical Introduction to PSL*, pp. 27–34, 2006.
- [55] A. Cimatti, M. Roveri, and D. Sheridan, “Bounded verification of past ltl,” in *International Conference on Formal Methods in Computer-Aided Design*. Springer, 2004, pp. 245–259.
- [56] H. Caesar, V. Bankiti, A. H. Lang, S. Vora, V. E. Liong, Q. Xu, A. Krishnan, Y. Pan, G. Baldan, and O. Beijbom, “nusenes: A multi-modal dataset for autonomous driving,” in *Proceedings of the IEEE/CVF Conference on Computer Vision and Pattern Recognition*, 2020, pp. 11 621–11 631.
- [57] Motional. (2019) nuScenes dataset. Accessed: 2020-11-14. [Online]. Available: <https://www.nusenes.org/nusenes>
- [58] S. Aluru, “Quadrees and octrees,” in *Handbook of Data Structures and Applications*. Chapman and Hall/CRC, 2018, pp. 309–326.
- [59] M. Shneier, “Calculations of geometric properties using quadrees,” *Computer Graphics and Image Processing*, vol. 16, no. 3, pp. 296–302, 1981.

- [60] O. Bournez, O. Maler, and A. Pnueli, "Orthogonal polyhedra: Representation and computation," in *International Workshop on Hybrid Systems: Computation and Control*. Springer, 1999, pp. 46–60.
- [61] G. E. Fainekos, S. Sankaranarayanan, K. Ueda, and H. Yazarel, "Verification of automotive control applications using s-taliro," in *2012 American Control Conference (ACC)*. IEEE, 2012, pp. 3567–3572.
- [62] F. Yu, H. Chen, X. Wang, W. Xian, Y. Chen, F. Liu, V. Madhavan, and T. Darrell, "Bdd100k: A diverse driving dataset for heterogeneous multitask learning," in *Proceedings of the IEEE/CVF Conference on Computer Vision and Pattern Recognition*, 2020, pp. 2636–2645.
- [63] A. Balakrishnan, J. Deshmukh, B. Hoxha, T. Yamaguchi, and G. Fainekos, "Percemon: Online monitoring for perception systems," in *International Conference on Runtime Verification (RV)*, ser. LNCS, vol. 12974, 2021.
- [64] J. Anderson, M. Hekmatnejad, and G. Fainekos, "PyFoReL: A domain-specific language for formal requirements in temporal logic," in *IEEE 30th International Requirements Engineering Conference (RE)*, 2022.
- [65] C. Zhang, Z. Huang, H. Guo, L. Qin, M. H. Ang Jr, and D. Rus, "Smart-rain: A degradation evaluation dataset for autonomous driving in rain." 2021. [Online]. Available: <http://rain.smart.mit.edu/smartrain/>
- [66] M. Bijelic, T. Gruber, F. Mannan, F. Kraus, W. Ritter, K. Dietmayer, and F. Heide, "Seeing through fog without seeing fog: Deep multimodal sensor fusion in unseen adverse weather," in *The IEEE/CVF Conference on Computer Vision and Pattern Recognition (CVPR)*, June 2020.

APPENDIX A

APPENDIX: STPL FUTURE SYNTAX

The following definition introduces a future fragment of the introduced STPL syntax in Def. 4.1. Here, we restrict the grammar by including rules that enforce a formula to be an *Almost Arbitrarily Nesting Formula* as in Def. 4.3. Notice that in the following, the grammar rules force the expressions to be indexed to track the level of nesting in variant-quantifier operators.

Definition A.1 (STPL AAN Syntax for Discrete-Time Signal): Let V_x and V_o be sets of time variables and object ID variables, respectively. Let x be a vector of time variables, i.e., $x = [x_0, \dots, x_{n-1}]^T$, and id be a vector of object ID variables, i.e., $id = [id_0, \dots, id_{m-1}]^T$, and \mathcal{I} be any non-empty interval of $\mathbb{R}_{\geq 0}$ over time. The syntax for Spatio-Temporal Perception Logic (STPL) formulas is provided by the following grammar:

$$\begin{aligned}
\Phi_{i,j} &::= \exists id_i @ x_i. \Phi_{i,j}^{f,q} \mid x_i. \Phi_i^f \mid \exists id_i. \Phi_{i,j}^q \\
&\quad \top \mid \neg \Phi_{i,j} \mid \Phi_{i,j} \vee \Phi_{i,j} \mid \bigcirc \Phi_{i,j} \mid \Phi_{i,j} \mathcal{U} \Phi_{i,j} \mid \\
&\quad \bigcirc_{\mathcal{I}} \Phi_{i,j} \mid \Phi_{i,j} \mathcal{U}_{\mathcal{I}} \Phi_{i,j} \mid \tilde{\bigcirc}_{\mathcal{I}} \Phi_{i,j} \mid \Phi_{i,j} \tilde{\mathcal{U}}_{\mathcal{I}} \Phi_{i,j} \\
\Phi_{i,j}^{f,q} &::= \Phi_i^f \mid \Phi_{i,i}^q \mid \\
&\quad \top \mid \neg \Phi_{i,j}^{f,q} \mid \Phi_{i,j}^{f,q} \vee \Phi_{i,j}^{f,q} \mid \bigcirc \Phi_{i,j}^{f,q} \mid \Phi_{i,j}^{f,q} \mathcal{U} \Phi_{i,j}^{f,q} \mid \\
&\quad \bigcirc_{\mathcal{I}} \Phi_{i,j}^{f,q} \mid \Phi_{i,j}^{f,q} \mathcal{U}_{\mathcal{I}} \Phi_{i,j}^{f,q} \mid \tilde{\bigcirc}_{\mathcal{I}} \Phi_{i,j}^{f,q} \mid \Phi_{i,j}^{f,q} \tilde{\mathcal{U}}_{\mathcal{I}} \Phi_{i,j}^{f,q} \\
\Phi_i^f &::= \tau - x_i > t \mid \mathcal{F} - x_i > n \mid \Phi_{i+1,i} \mid \\
&\quad \top \mid \neg \Phi_i^f \mid \Phi_i^f \vee \Phi_i^f \mid \bigcirc \Phi_i^f \mid \Phi_i^f \mathcal{U} \Phi_i^f \mid \\
&\quad \bigcirc_{\mathcal{I}} \Phi_i^f \mid \Phi_i^f \mathcal{U}_{\mathcal{I}} \Phi_i^f \mid \tilde{\bigcirc}_{\mathcal{I}} \Phi_i^f \mid \Phi_i^f \tilde{\mathcal{U}}_{\mathcal{I}} \Phi_i^f \\
\Phi_{i,j}^q &::= C(\Lambda_{i,j}) == c \mid C(\Lambda_{i,j}) == C(\Lambda_{i,j}) \mid P(\Lambda_{i,j}) \geq r \\
&\quad \mid P(\Lambda_{i,j}) \geq r \times P(\Lambda_{i,j}) \mid \Lambda_{i,j} == \Lambda_{i,j} \mid \Phi_{i+1,j} \mid \\
&\quad \top \mid \neg \Phi_{i,j}^q \mid \Phi_{i,j}^q \vee \Phi_{i,j}^q \mid \bigcirc \Phi_{i,j}^q \mid \Phi_{i,j}^q \mathcal{U} \Phi_{i,j}^q \mid \\
&\quad \bigcirc_{\mathcal{I}} \Phi_{i,j}^q \mid \Phi_{i,j}^q \mathcal{U}_{\mathcal{I}} \Phi_{i,j}^q \mid \tilde{\bigcirc}_{\mathcal{I}} \Phi_{i,j}^q \mid \Phi_{i,j}^q \tilde{\mathcal{U}}_{\mathcal{I}} \Phi_{i,j}^q \mid \\
&\quad \exists \Omega_{i,j} \mid \Theta_{i,j} \mid \Pi_{i,j} \\
\Lambda_{i,j} &::= id_j \mid id_{j+1} \mid \dots \mid id_i \\
\Omega_{i,j} &::= \mathcal{C}(\Lambda_{i,j}) \mid \emptyset \mid \mathbb{U} \mid \bar{\Omega}_{i,j} \mid \Omega_{i,j} \sqcap \Omega_{i,j} \mid \mathbf{I}\Omega_{i,j} \mid \\
&\quad \Omega_{i,j} \mathcal{U}_s \Omega_{i,j} \mid \diamond_s \Omega_{i,j} \mid \square_s \Omega_{i,j} \mid \bigcirc_s \Omega_{i,j} \mid \\
&\quad \Omega_{i,j} \mathcal{U}_{s,\mathcal{I}} \Omega_{i,j} \mid \diamond_{s,\mathcal{I}} \Omega_{i,j} \mid \square_{s,\mathcal{I}} \Omega_{i,j} \mid \bigcirc_{s,\mathcal{I}} \Omega_{i,j} \mid \\
&\quad \Omega_{i,j} \tilde{\mathcal{U}}_{s,\mathcal{I}} \Omega_{i,j} \mid \tilde{\diamond}_{s,\mathcal{I}} \Omega_{i,j} \mid \tilde{\square}_{s,\mathcal{I}} \Omega_{i,j} \mid \tilde{\bigcirc}_{s,\mathcal{I}} \Omega_{i,j} \\
\Pi_{i,j} &::= Area(\Omega_{i,j}) \geq r \mid Area(\Omega_{i,j}) \geq r \times Area(\Omega_{i,j})
\end{aligned}$$

$$\begin{aligned}
\Theta_{i,j} &::= Dist(\Lambda_{i,j}, CRT, \Lambda_{i,j}, CRT) \geq r \mid \\
&\quad Lat(\Lambda_{i,j}, CRT) \geq r \mid Lon(\Lambda_{i,j}, CRT) \geq r \mid \\
&\quad Lat(\Lambda_{i,j}, CRT) \geq r \times Lat(\Lambda_{i,j}, CRT) \mid \\
&\quad Lon(\Lambda_{i,j}, CRT) \geq r \times Lon(\Lambda_{i,j}, CRT) \mid \\
&\quad Lat(\Lambda_{i,j}, CRT) \geq r \times Lon(\Lambda_{i,j}, CRT) \mid \\
&\quad Area(\Lambda_{i,j}) \geq r \mid Area(\Lambda_{i,j}) \geq r \times Area(\Lambda_{i,j})
\end{aligned}$$

$$CRT ::= LM \mid RM \mid TM \mid BM \mid CT$$

where $i \geq 0$, and the grammar starts from $\Phi_{0,0}$.

The time and frame constraints of STPL are represented in the form of $\tau - x > r$ and $\mathcal{F} - x > n$, respectively. The freeze time quantifier $x.\phi$ assigns the current frame i to time variable x before processing the subformula ϕ . The *Existential* quantifier is denoted as \exists , and the *Universal* quantifier is denoted as \forall . The following syntactic equivalences hold for the STPL formulas ψ and ϕ using syntactic manipulation. $\forall \{id\} @ x. \phi \equiv \neg(\exists \{id\} @ x. \neg \phi)$, $\psi \wedge \phi \equiv \neg(\neg \psi \vee \neg \phi)$, $\perp \equiv \neg \top$ (False), $\psi \rightarrow \phi \equiv \neg \psi \vee \phi$ (ψ Implies ϕ), $\phi \mathcal{R} \psi \equiv \neg(\neg \phi \mathcal{U} \neg \psi)$ (ϕ releases ψ), $\phi \bar{\mathcal{R}} \psi \equiv \phi \mathcal{R} (\phi \vee \psi)$ (ϕ non-strictly releases ψ), $\diamond \psi \equiv \top \mathcal{U} \psi$ (Eventually ψ), $\square \psi \equiv \neg \diamond \neg \psi$ (Always ψ).

For parsing a formula using the above grammar, there are two production rules Φ_i^f and $\Phi_{i,j}^q$ in which we can use the initial production rule after increasing the index i (i.e., $\Phi_{i+1,j}$). The index i is to force scope for the use of freeze time variables. For example, if in the scope of a variant-quantifier operator we use x_0 , then the index will increase to 1 to avoid use of x_0 in the scope of the next variant-quantifier operator. The index j is used as a pointer to each quantifier operator to track the scope of ID variables. For example, in the formula $\varphi \equiv \exists id_0. \square(\exists id_1. \exists id_2. (\phi_1) \vee \phi_2)$, we have $i = 2$ and $j = 0$ while parsing the subformula ϕ_1 , whereas, in ϕ_2 , we have $i = 0$ and $j = 0$. Thus any function in ϕ_1 with ID variables in it will use the production rule $\Lambda_{2,0}$. Thus, the allowed ID variables in ϕ_1 are id_0, id_1 and id_2 . However, while parsing the subformula ϕ_2 , we use $\Lambda_{0,0}$ in which the only allowed ID variable is id_0 .

APPENDIX B

APPENDIX: MONITORING ALGORITHM

Here, we are going to explain the monitoring algorithm (that works with the future fragment of the STPL syntax) using the below formula presented before in Eq. (13).

$$\begin{aligned}
\varphi &:= \square \forall Id_1 @ x. \square \exists Id_2. \left(\left(\bigvee (\bar{\mathcal{C}}(Id_1) \sqcup \mathcal{C}(Id_2)) \right) \wedge \right. \\
&\quad \left. \bigvee (\bar{\mathcal{C}}(Id_2) \sqcup \mathcal{C}(Id_1)) \right) \wedge Id_1 == Id_2
\end{aligned}$$

A. Algorithm-1

This algorithm represents the main dynamic programming body of the monitoring algorithm. It receives an STPL formula φ , data stream $\hat{\rho}$, and dynamic programming tables M and F . The formula is divided into subformulas as stated in Figure 12. We clustered a formula into subsections each represented by a

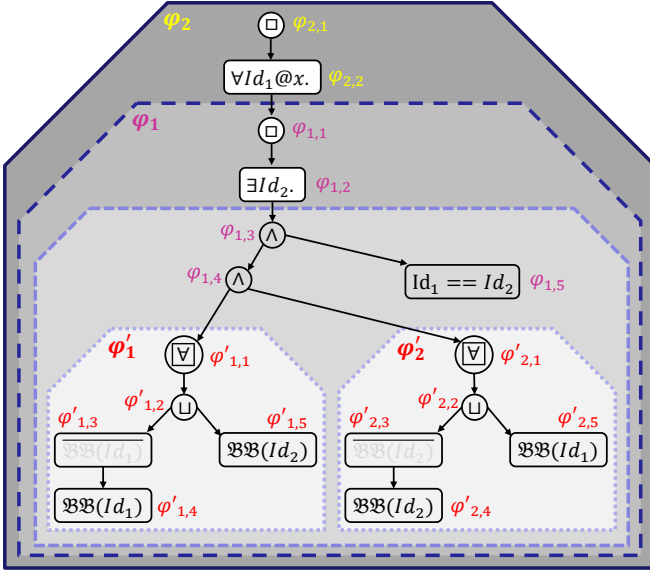


Fig. 12: A parse tree for the formula in Eq. 13. Distinct regions represent subformulas φ_2 , φ_1 , φ'_1 , and φ'_2 . In each region, the subformulas subscript into the operators and predicates levels.

freeze operator as φ_1 in Fig. 12. In addition, the whole formula represents the root cluster as φ_2 in Fig. 12, despite the fact if it has or does not have a freeze operator in the beginning. The freeze operator clusters get subindex numbers relevant to their appearance order in the formula. The second subindex of each cluster denotes its evaluating order (e.g., preorder traverse) on the tree. For the spatio-temporal formula, we use new symbol φ' with the same indexing idea except that we do not expect freeze operators in them.

The main loops in the algorithm are nested starting from line 5. The first loop over the number of freeze time operators is to evaluate each cluster of the formula from the deepest one until before the root (i.e., φ_1 assigns 1 to the variable k). As one can see, we compute the root cluster after the end of the first nested loop starting at line 20. The second nested loop starting at 22 does exactly the same as the first nested loop, except without considering the freeze frame variables. The second loop starts at line 6 and assigns frame numbers to t as the freeze frame variable which we denoted in the STPL semantics as ϵ function. The third loop starts at line 7 and uses the variable u as a counter for the current evaluating frame, and it starts from the last frame to the last frozen frame t . The last loop starts at line 8 and iterates over the subindexes of the formulas in each cluster k . In this loop, we check if the k 'th subformula is an spatio-temporal formula or it is not. I will pass it to the algorithm 3 if it was a spatio-temporal formula, otherwise, we will use the algorithm 2. We used variables u_{01} and t_{01} to alternate between the current and next columns of the Dynamic Programming (DP) tables M and F , respectively. These tables store the result of evaluating each subformula at each frame u . In the end, the algorithm stores the final evaluation result in $M[1, u_{01}]$. For building our DP tables, we only need the values of the current and the next frames rather than all of the frames.

B. Algorithm-2

This algorithm computes the values of the DP table M as defined in the temporal semantics of the STPL logic in Def. IV-B1. For a given subformula, first it determines the operator and then fills the current columns of the DP tables accordingly. Most of the lines of the algorithm are straightforward where there is no DP table F in the assignments. The idea of using the separate DP table F for the freeze subformulas is to store the result of their evaluating at each frozen time, and then update the DP table M using them accordingly. Table M has two columns for each subformula, one for the current time and the other for the next time. We use u_{01} and u_{10} to refer to the current column (current frame) for updating and the next column (next frame) for reading, respectively. Therefore, we need to toggle the value of these variables (between 0 and 1) to change the read column to write column and vice versa. Table F has two rows for each frame, one for the current time and the other for the next time. We use t_{01} and t_{10} to refer to the current row for updating and the next row for reading, respectively. Therefore, we need to toggle the value of these variables (between 0 and 1) to change the read row to write row and vice versa. The $M[j, u_{01}].val$ data-member of the DP table M keeps the current evaluating result of the j 'th subformula φ_j at the current frame. The other data-members are used to update *min/max* values for the quantifier operators. The *IT* data-member is a table of size $(S_O)^{|V_{id}|}$, where S_O is the maximum number of objects in all input frames, and V_{id} is the set of the *Id* variables in the scope of the evaluating subformula φ_j .

C. Algorithm-3

This algorithm computes the identifier table *IT* values of the DP table M . Here, we compute spatial functions and quantifier operations. For a given spatial function $Fn(\dots)$, if it has nested function operators, then this algorithm recursively computes the final values. The *IT* table stores the values for any functional expression based on the combinatorial assignments of objects to the ID variables. In line 9, if the combination of IDs do not satisfy the correct range of existing objects in the current frame or a frozen frame, then it assigns $-\infty$ (or bottom \perp) to it. Otherwise, if any parameter is a spatial formula, then it runs algorithm 5 or 4 depending on if the spatial formulas have frame-interval operators in them or not, respectively. The size of the *IT* table is the maximum number of combinations for objects with respect to the ID variables. For example, if there are maximum five objects per frames in an object stream, and a formula has a maximum of three nested ID variables in it, then the size of *IT* is $5^3 = 125$. We choose the size of the *IT* table based on the worst case scenario, but for an efficient computation, we only compute as many as needed combinations for each quantifier subformula based on its scope. Therefore, we mark the remaining cells of the table with NaN for extended computation that merges these tables for different subformulas in Algorithm 2 by calling function *UpdateIdTable* at line 24.

Algorithm 1 STPL Monitor

Input: $\varphi, \hat{\rho} = (\sigma_0, \tau_0)(\sigma_1, \tau_1) \dots (\sigma_T, \tau_T)$; **Global variables:** $M_{|\varphi| \times 2, F_{2 \times |\hat{\rho}|}}$; **Output:** $M[1, 0]$.

procedure STPL-MONITOR($\varphi, \hat{\rho}$)

- 1: $u_{01} \leftarrow 0$ and $t_{01} \leftarrow 0$ \triangleright toggle between 0 and 1
- 2: $\varphi' \leftarrow$ set of all the spatio-temporal operators in φ \triangleright i.e., $\exists, \forall, Area, LAT$, and so forth
- 3: $\overline{M}_{|\varphi'| \times 2}$ is a table dedicated to the spatial subformulas
- 4: $V \leftarrow$ all freeze time variables in φ
- 5: **for** $k \leftarrow 1$ to $|V|$ **do** \triangleright iterates over time variables
- 6: **for** $t \leftarrow 0$ to $|\hat{\rho}| - 1$ **do** \triangleright iterates over time stamps
- 7: **for** $u \leftarrow |\hat{\rho}| - 1$ down to t **do** \triangleright iterates backward over time stamps
- 8: **for** $j \leftarrow \varphi_k.max$ down to $\varphi_k.min$ **do** \triangleright iterates over subformulas in each frozen cluster
- 9: **if** $\varphi_k \in \varphi'$ **then**
- 10: $ComputeFnExpr(\varphi, k, u, u_{01}, t, \hat{\rho}, M, \overline{M})$
- 11: **else**
- 12: $ComputeLTL(\varphi_j, u, u_{01}, t, t_{01}, k, M, F)$
- 13: **end if**
- 14: **end for**
- 15: $u_{01} \leftarrow toggle(u_{01})$
- 16: **end for**
- 17: $u_{01} \leftarrow toggle(u_{01})$
- 18: **end for**
- 19: **end for**
- 20: $k \leftarrow |V| + 1$
- 21: **if** φ_k is not a freeze operator **then**
- 22: **for** $u \leftarrow |\hat{\rho}| - 1$ down to 0 **do**
- 23: **for** $j \leftarrow \varphi_k.max$ down to $\varphi_k.min$ **do**
- 24: **if** $\varphi_k \in \varphi'$ **then**
- 25: $ComputeFnExpr(\varphi, k, u, u_{01}, t, \hat{\rho}, M, \overline{M})$
- 26: **else**
- 27: $ComputeLTL(\varphi_j, u, u_{01}, 0, t_{01}, 0, M, F)$
- 28: **end if**
- 29: **end for**
- 30: $u_{01} \leftarrow toggle(u_{01})$
- 31: **end for**
- 32: $u_{01} \leftarrow toggle(u_{01})$
- 33: **else**
- 34: $u_{01} \leftarrow toggle(u_{01})$, $t_{01} \leftarrow toggle(t_{01})$
- 35: $M[1][u_{01}] = F[t_{01}][0]$
- 36: **end if**
- 37: **return** $M[1, u_{01}]$

end procedure

D. Algorithm-4

This algorithm computes the values of the DP table \overline{M} . It computes spatial formulas similar to algorithm 2 except that here there are spatial operation functions that calculate set-based results. We do not present the algorithms for these functions as they can be implemented with various data structures as simply as a linked list to as efficient as quadrees and octrees. Algorithm 5 is the same as Algorithm 4, except that the spatio-temporal operators can take frame/time intervals.

APPENDIX C

APPENDIX: COMPLEXITY ANALYSIS

Let assume that we use the linked-list data structure to represent a spatial term \mathcal{T} as a union of a finite number of unique subsets. We can compute $\mathfrak{M}(\tau_1 \mathcal{U}_{\mathcal{T}}^s \tau_2, t)$ recursively as $\mathfrak{M}(\tau_2, t) \cup (\mathfrak{M}(\tau_1, t) \cap \mathfrak{M}((\tau_1 \mathcal{U}_{\mathcal{T}}^s \tau_2, t + 1)))$. For each until formula in each row of Table IV (starting from the row $l = 1$), for each time step t , we use the recursive evaluation function to calculate the maximum number of bounding boxes as a result of computing the formula. The maximum number of bounding boxes that can be produced by $\tau_1 \cup \tau_2$ is equal

Algorithm 2 LTL Monitor

Input: $\varphi_j, u, u_{01}, t, t_{01}, j, M_{|\varphi| \times 2, F_{2 \times |\hat{\rho}|}}$; **Output:** $M[j, u_{01}]$.

procedure COMPUTELTL($\varphi_j, u, u_{01}, t, t_{01}, j, M_{|\varphi| \times 2, F_{2 \times |\hat{\rho}|}}$)

- 1: $u_{10} \leftarrow toggle(u_{01}), t_{10} \leftarrow toggle(t_{01})$
- 2: **if** $\varphi_j \equiv p \in AP$ **then**
- 3: $M[j, u_{01}].val \leftarrow \llbracket p \rrbracket(\hat{\rho}, u)$
- 4: **else if** $\varphi_j \equiv \tau - v_k \sim r$ **then**
- 5: **if** $(\tau_u - \tau_t) \sim r$ **then**
- 6: $M[j, u_{01}].val \leftarrow +\infty$
- 7: **else**
- 8: $M[j, u_{01}].val \leftarrow -\infty$
- 9: **end if**
- 10: **else if** $\varphi_j \equiv \mathcal{F} - v_k \sim r$ **then**
- 11: **if** $(u - t) \sim r$ **then**
- 12: $M[j, u_{01}].val \leftarrow +\infty$
- 13: **else**
- 14: $M[j, u_{01}].val \leftarrow -\infty$
- 15: **end if**
- 16: **else if** φ_j is a freeze subformula **then**
- 17: $M[j, u_{01}] \leftarrow M[j + 1, u_{01}]$
- 18: **if** φ_j has an \exists quantifier **then**
- 19: $M[j, u_{01}].val \leftarrow M[j, u_{01}].max$
- 20: **else**
- 21: $M[j, u_{01}].val \leftarrow M[j, u_{01}].min$
- 22: **end if**
- 23: $F[t_{01}][t] \leftarrow M[j, u_{01}]$
- 24: $UpdateIdTable(M[j, u_{01}].IT)$
- 25: **else if** $\varphi_j \equiv \neg \varphi_m$ **then**
- 26: $M[j, u_{01}].val = -M[m, u_{01}].val$
- 27: $M[j, u_{01}].min \leftarrow -M[m, u_{01}].max$
- 28: $M[j, u_{01}].max \leftarrow -M[m, u_{01}].min$
- 29: $M[j, u_{01}].IT \leftarrow -M[j, u_{01}].IT$
- 30: **else if** $\varphi_j \equiv \varphi_m \vee \varphi_n$ **then**
- 31: $M[j, u_{01}] \leftarrow \max(M[m, u_{01}], M[n, u_{01}])$
- 32: **else if** $\varphi_j \equiv \bigcirc \varphi_m$ **then**
- 33: **if** $u = |\hat{\rho}| - 1$ **then**
- 34: $M[j, u_{01}] \leftarrow -\infty$
- 35: **else if** φ_m is followed by $@\{x, \dots\}$ **then**
- 36: $M[j, u_{01}] \leftarrow F[t_{10}, u + 1]$
- 37: **else**
- 38: $M[j, u_{01}] \leftarrow M[m, u_{10}]$
- 39: **end if**
- 40: **else if** $\varphi_j \equiv \varphi_m \mathcal{U} \varphi_n$ **then**
- 41: **if** $u = |\hat{\rho}| - 1$ **then**
- 42: $M[j, u_{01}] \leftarrow M[n, u_{01}]$
- 43: **else**
- 44: **if** φ_m is followed by x . **then**
- 45: $M[m, u_{01}] \leftarrow F[t_{10}, u]$
- 46: **end if**
- 47: **if** φ_n is followed by x . **then**
- 48: $M[n, u_{01}] \leftarrow F[t_{10}, u]$
- 49: **end if**
- 50: $M[j, u_{01}] \leftarrow \max(M[n, u_{01}], \min(M[m, u_{01}], M[j, u_{10}]))$
- 51: **end if**
- 52: **end if**

end procedure

to the total number of boxes in the two spatial terms (i.e., $|\tau_1| + |\tau_2|$). Additionally, the maximum number of bounding boxes that can be produced by $\tau_1 \cap \tau_2$ is equal to the product of number of boxes in the two spatial terms (i.e., $|\tau_1| \times |\tau_2|$). Consequently, the maximum number of bounding boxes that can be produced at each time step t for the above until formula is $|\mathfrak{M}(\tau_2, t)| + |\mathfrak{M}(\tau_1, t)| \times |\mathfrak{M}(\tau_1 \mathcal{U}_{\mathcal{T}}^s \tau_2, t + 1)|$.

A. Formulas with Exponential Time/Space Complexities

As it is stated in the first and second rows in Table IV, the number of needed operations grow as in arithmetic sequences. Thus, the time complexity which is the summation of numbers

Algorithm 3 Compute Function Expression

Input: $\varphi, k, u, u_{01}, t, \hat{\rho}, M_{|\varphi| \times 2}, \bar{M}_{|\varphi| \times 2}$; **Output:** $M[k, u_{01}]$.

procedure COMPUTEFNEXPR($\varphi, k, u, u_{01}, t, \hat{\rho}, M_{|\varphi| \times 2}, \bar{M}_{|\varphi| \times 2}$)

- 1: $\varphi_k \equiv Fn(\Omega_1, \dots, \Omega_n) \sim r$ where
 $r \in \mathbb{R}, \sim \in \{>, <, \geq, \leq, ==, !=\}$,
and Fn is a reserved function name
- 2: $P_{n \times 1}$ is a list used to store the evaluated arguments of Fn
- 3: $S_{id} \leftarrow (S_O)^{|V_{id}|}$ where
 S_O is the maximum number of objects in all the frames
and V_{id} is the set of the ID variables in the scope of φ_k
- 4: $S_O^{cf} \leftarrow$ number of objects in the current frame u
- 5: $S_O^{ff} \leftarrow$ number of the objects in the freeze frame t
- 6: $F_{ID} \leftarrow$ is a map s.t.
 $\forall Id \in V_{id}, \{F_{ID}[Id] = true \mid \exists " \exists Id @ v_x. " \in \varphi$
or $" \forall Id @ v_x. " \in \varphi\}$, $v_x \in V_{id}$
- 7: **for** $i \leftarrow 1$ **to** S_{id} **do** \triangleright iterates over combinatorial assignments of values to the IDs
- 8: $\{Id_1, \dots, Id_{|V_{id}|}\} \leftarrow$ i'th combinatorial of $\{1, \dots, S_O\}$
to $\{Id_j \mid Id_j \in V_{id}, 1 \leq j \leq |V_{id}|\}$
- 9: **if** $\exists Id \in V_{id}$ and $((F_{ID}[Id] == true \text{ and } Id > S_O^{ff}) \text{ or } (F_{ID}[Id] == false \text{ and } Id > S_O^{cf}))$ **then**
- 10: $M[k, u_{01}].IT[i-1] \leftarrow -\infty$
- 11: **else**
- 12: **for** $j \leftarrow 1$ **to** n **do** \triangleright iterates over Fn arguments
- 13: **if** Ω_j is a const number or reserved word **then**
- 14: $P[j].val \leftarrow \Omega_j$
- 15: **else if** $\Omega_j \equiv Fn(\dots)$ **then**
- 16: $P[j].val \leftarrow$
 $ComputeFnExpr(\Omega_j, k, u, u_{01}, t, \hat{\rho}, M, \bar{M})$
- 17: **else if** $\Omega_j \equiv C(Id)$ **then**
- 18: $P[j].region \leftarrow BoundingBox(Id, F_{ID}, u, t)$
- 19: **else if** Ω_j is a spatial formula **then**
- 20: $P[j].region \leftarrow$
 $ComputeSpatioTemporal(\Omega_j, u, t, i, \hat{\rho}, \bar{M}, F_{ID})$
- 21: **end if**
- 22: **end for**
- 23: $M[k, u_{01}].IT[i-1] \leftarrow ComputeRobust(Fn, P, \sim, r)$
- 24: **end if**
- 25: **end for**
- 26: $S_{ID} \leftarrow (S_O)^L$ where
 L is the maximum number of Id variables that can be used
in the scope of any $@\{\dots\}$ subformula
- 27: **for** $i \leftarrow S_{id}$ **to** $S_{ID} - 1$ **do** \triangleright iterates over the remaining of the ID Table
- 28: $M[k, u_{01}].IT[i] \leftarrow \text{NaN}$
- 29: **end for**
- end procedure**

in the rows, are linear and polynomial functions of the number of the time steps for the first and second rows, respectively. Moreover, the space complexity for the first and the second rows are constant and linear functions of number of the time steps, respectively.

In the following, we calculate an upper bound and a lower bound for the maximum number of bounding boxes that can be produced for the third row (level 2) of the until operator. We use the function $f_2(t)$ to denote the maximum number of bounding boxes that are produced at the time step t for the until formula $(\tau \mathcal{U}_L^s \tau) \mathcal{U}_L^s (\tau \mathcal{U}_L^s \tau)$.

$$\sum_{t=1}^n f_2(t) =$$

$$1 + 2(1+1) + 3(1+2(1+1)) +$$

$$4(1+3(1+2(1+1))) + 5(1+4(1+3(1+2(1+1)))) + \dots$$

$$+ n(1+(n-1)(1+(n-2)(\dots 1+2(1+1)))) \dots \quad (20)$$

We repetitively use the inequality $(a+1)b > a(1+b)$ for $b > a$

Algorithm 4 Spatio-Temporal Monitor (no-interval)

Input: $\theta, u', t, i, \hat{\rho}, \bar{M}_{|\varphi'| \times 2}, F_{ID}$; **Output:** $\bar{M}[\theta.min, u_{01}]$.

procedure COMPUTESPATIOTEMPORAL($\theta, u', t, i, \hat{\rho}, \bar{M}_{|\varphi'| \times 2}, F_{ID}$)

- 1: $u_{01} \leftarrow 0$ \triangleright local index variable for current time
- 2: $u_{10} \leftarrow toggle(u_{01})$ \triangleright local index variable for next time
- 3: $\{Id_1, \dots, Id_{|V_{id}|}\} \leftarrow$ i'th combinatorial assignment of $\{1, \dots, S_O\}$ to ID variables
- 4: **for** $u \leftarrow |\hat{\rho}| - 1$ **down to** u' **do** \triangleright iterates backward over time stamps
- 5: $S_O^{cf} \leftarrow$ number of objects in the current frame u
- 6: $S_O^{ff} \leftarrow$ number of the objects in the freeze frame t
- 7: **for** $j \leftarrow \theta.max$ **down to** $\theta.min$ **do** \triangleright iterates over subformulas
- 8: **if** $\varphi_j \equiv C(Id)$ **then**
- 9: **if** $((F_{ID}[Id] == true \text{ and } Id > S_O^{ff}) \text{ or } (F_{ID}[Id] == false \text{ and } Id > S_O^{cf}))$ **then**
- 10: $\bar{M}[j, u_{01}] \leftarrow \emptyset$ \triangleright mark as NaN
- 11: **else**
- 12: $\bar{M}[j, u_{01}] \leftarrow BoundingBox(Id, F_{ID}, u, t)$
- 13: **end if**
- 14: **else if** $\varphi_j \equiv \bar{\varphi}_m$ **then**
- 15: $\bar{M}[j, u_{01}] \leftarrow Complement(\bar{M}[m, u_{01}])$
- 16: **else if** $\varphi_j \equiv \varphi_m \sqcap \varphi_n$ **then**
- 17: $\bar{M}[j, u_{01}] \leftarrow Intersection(\bar{M}[m, u_{01}], \bar{M}[n, u_{01}])$
- 18: **else if** $\varphi_j \equiv \varphi_m \sqcup \varphi_n$ **then**
- 19: $\bar{M}[j, u_{01}] \leftarrow Union(\bar{M}[m, u_{01}], \bar{M}[n, u_{01}])$
- 20: **else if** $\varphi_j \equiv \mathbf{I} \varphi_m$ **then**
- 21: $\bar{M}[j, u_{01}] \leftarrow Interior(\bar{M}[m, u_{01}])$
- 22: **else if** $\varphi_j \equiv \mathbf{C} \varphi_m$ **then**
- 23: $\bar{M}[j, u_{01}] \leftarrow Closure(\bar{M}[m, u_{01}])$
- 24: **else if** $\varphi_j \equiv \mathbf{O}^s \varphi_m$ **then**
- 25: **if** $u = |\hat{\rho}| - 1$ **then**
- 26: $\bar{M}[j, u_{01}] \leftarrow \emptyset$
- 27: **else**
- 28: $\bar{M}[j, u_{01}] \leftarrow \bar{M}[m, u_{10}]$
- 29: **end if**
- 30: **else if** $\varphi_j \equiv \varphi_m \mathcal{U}^s \varphi_n$ **then**
- 31: **if** $u = |\hat{\rho}| - 1$ **then**
- 32: $\bar{M}[j, u_{01}] \leftarrow \bar{M}[n, u_{01}]$
- 33: **else**
- 34: $\bar{M}[j, u_{01}] \leftarrow \bar{M}[n, u_{01}] \sqcup$
 $(\bar{M}[m, u_{01}] \sqcap \bar{M}[j, u_{10}])$
- 35: **end if**
- 36: **end if**
- 37: **end for**
- 38: $u_{01} \leftarrow toggle(u_{01})$
- 39: **end for**
- 40: $u_{01} \leftarrow toggle(u_{01})$
- 41: **return** $\bar{M}[\theta.min, u_{01}]$
- end procedure**

to derive the following inequality from the above equation

$$\sum_{t=1}^n f_2(t) < 1 + 3! + 4! + 5! + 6! + \dots + (n+1)! \quad (21)$$

where $n \geq 2$. Therefore, we have

$$\sum_{t=1}^n f_2(t) < n \times (n+1)! < (n+2)! \quad (22)$$

Next, we calculate a lower bound for the maximum number of bounding boxes that can be produced for the level 2 of the until operator. We repetitively use the inequality $2^{(b+1)} < a(1+2^b)$ for $a \geq 2$ to derive the following inequality from Eq. (20)

$$\sum_{t=1}^n f_2(t) > 1 + 2^1 + 2^2 + 2^3 + 2^4 + \dots + 2^{(n-1)} \quad (23)$$

Algorithm 5 Spatio-Temporal Monitor (with intervals)

Input: $\theta, u', t, i, \hat{\rho}, \bar{M}_{|\varphi'| \times |\hat{\rho}|}, F_{ID}$; **Output:** $\bar{M}[\theta.min, u_{01}]$.

```

procedure COMPUTESPATIOTEMPORAL( $\theta, u', t, i, \hat{\rho}, \bar{M}_{|\varphi'| \times |\hat{\rho}|}, F_{ID}$ )
1:  $u_{01} \leftarrow u$  ▷ local index variable for current time
2:  $u_{10} \leftarrow u + 1$  ▷ local index variable for next time
3:  $\{Id_1, \dots, Id_{|V_{id}|}\} \leftarrow i$ 'th combinatorial assignment of  $\{1, \dots, S_O\}$  to Id variables
4: for  $u \leftarrow |\hat{\rho}| - 1$  down to  $u'$  do ▷ iterates backward over time stamps
5:    $S_O^{cf} \leftarrow$  number of objects in the current frame  $u$ 
6:    $S_O^{ff} \leftarrow$  number of the objects in the freeze frame  $t$ 
7:   for  $j \leftarrow \theta.max$  down to  $\theta.min$  do ▷ iterates over subformulas
8:     if  $\varphi_j \in \mathcal{C}(Id)$  then
9:       if  $((F_{ID}[Id] == true \text{ and } Id > S_O^{ff}) \text{ or } (F_{ID}[Id] == false \text{ and } Id > S_O^{cf}))$  then
10:          $\bar{M}[j, u_{01}] \leftarrow \emptyset$  ▷ mark as NaN
11:       else
12:          $\bar{M}[j, u_{01}] \leftarrow \text{BoundingBox}(Id, F_{ID}, u, t)$ 
13:       end if
14:     else if  $\varphi_j \equiv \bar{\varphi}_m$  then
15:        $\bar{M}[j, u_{01}] \leftarrow \text{Complement}(\bar{M}[m, u_{01}])$ 
16:     else if  $\varphi_j \equiv \varphi_m \sqcap \varphi_n$  then
17:        $\bar{M}[j, u_{01}] \leftarrow \text{Intersection}(\bar{M}[m, u_{01}], \bar{M}[n, u_{01}])$ 
18:     else if  $\varphi_j \equiv \varphi_m \sqcup \varphi_n$  then
19:        $\bar{M}[j, u_{01}] \leftarrow \text{Union}(\bar{M}[m, u_{01}], \bar{M}[n, u_{01}])$ 
20:     else if  $\varphi_j \equiv \mathbf{I} \varphi_m$  then
21:        $\bar{M}[j, u_{01}] \leftarrow \text{Interior}(\bar{M}[m, u_{01}])$ 
22:     else if  $\varphi_j \equiv \mathbf{C} \varphi_m$  then
23:        $\bar{M}[j, u_{01}] \leftarrow \text{Closure}(\bar{M}[m, u_{01}])$ 
24:     else if  $\varphi_j \equiv \varphi_m \tilde{\mathcal{U}}_{\mathcal{I}} \varphi_n$  then
25:       if  $u = |\hat{\rho}| - 1$  and  $0 \in \mathcal{I}$  then
26:          $\bar{M}[j, u_{01}] \leftarrow \bar{M}[n, u_{01}]$ 
27:       else if  $u = |\hat{\rho}| - 1$  and  $0 \notin \mathcal{I}$  then
28:          $\bar{M}[j, u_{01}] \leftarrow \perp$ 
29:       else if  $\mathcal{I} = [0, +\infty)$  then
30:          $\bar{M}[j, u_{01}] \leftarrow \bar{M}[n, u_{01}] \sqcup (\bar{M}[m, u_{01}] \sqcap \bar{M}[j, u_{10}])$ 
31:       else
32:          $b_l \leftarrow \min\{j + \mathcal{I}\}; b_u \leftarrow \max\{j + \mathcal{I}\}$ 
33:          $r_{min} \leftarrow \sqcap_{j \leq j' < b_l} \bar{M}[m, j']$ 
34:          $\bar{M}[j, u] \leftarrow \perp$ 
35:         for  $j' \leftarrow b_l$  to  $b_u$  do ▷ iterates over frame indices
36:            $\bar{M}[j, j'] \leftarrow \bar{M}[j, j'] \sqcup (\bar{M}[n, j'] \sqcap r_{min})$ 
37:            $r_{min} \leftarrow r_{min} \sqcap \bar{M}[m, j']$ 
38:         end for
39:         if  $\sup \mathcal{I} == +\infty$  then
40:            $\bar{M}[j, u] \leftarrow \bar{M}[j, u] \sqcup (\bar{M}[m, u] \sqcap \bar{M}[j, u + 1])$ 
41:         end if
42:       end if
43:     end if
44:   end for
45:    $u_{01} \leftarrow \text{toggle}(u_{01})$ 
46: end for
47:  $u_{01} \leftarrow \text{toggle}(u_{01})$ 
48: return  $\bar{M}[\theta.min, u_{01}]$ 
end procedure

```

where $n \geq 2$. Therefore, we have

$$\sum_{t=1}^n f_2(t) > 2^n \quad (24)$$

This time inequality suggests that the time/space complexity for any formulas with more than one level of nesting can be exponential.

B. Best Complexity for the Worst Formulas

We can repeat the above method to calculate a lower bound for each row of the table by using the inequality $a^{r+1} < a^r(1 +$

l	t_n	t_{n-1}	t_{n-2}	t_{n-3}	t_{n-4}	\dots
0	1	1	1	1	1	\dots
1	1	$1(1+1) = 2$	$1(1+1(1+1)) = 3$	$1(1+1(1+1(1+1))) = 4$	$1(1+1(1+1(1+1(1+1)))) = 5$	\dots
2	1	$2(1+1) = 4, 2 \leq 4 \leq 3!$	$3(1+2(1+1)) = 15, 2^2 \leq 15 \leq 4!$	$4(1+3(1+2(1+1))) = 64, 2^3 \leq 64 \leq 5!$	$5(1+4(1+3(1+2(1+1)))) = 325, 2^4 \leq 325 \leq 6!$	\dots
3	1	$2(1+1(1+1)) = 8$	$3(1+2(1+1(1+1))) = 135$	$4(1+3(1+2(1+1(1+1)))) = 8,704$	$5(1+4(1+3(1+2(1+1(1+1)))) = 2,829,125$	\dots
\dots	\dots	\dots	\dots	\dots	\dots	\dots

TABLE IV: DP-based complexity analysis for spatio-temporal until operator with different levels of nesting. At $l = 0$ we have $\tau = \mathcal{C}(Id)$; At $l = 1$: we have $\tau \mathcal{U}_{\mathcal{I}}^s \tau$, and $\tau \mathcal{U}_{\mathcal{I}}^s \tau$; At $l = 2$: we have $(\tau \mathcal{U}_{\mathcal{I}}^s \tau) \mathcal{U}_{\mathcal{I}}^s (\tau \mathcal{U}_{\mathcal{I}}^s \tau)$; Finally, at $l = 3$: we have $((\tau \mathcal{U}_{\mathcal{I}}^s \tau) \mathcal{U}_{\mathcal{I}}^s (\tau \mathcal{U}_{\mathcal{I}}^s \tau)) \mathcal{U}_{\mathcal{I}}^s ((\tau \mathcal{U}_{\mathcal{I}}^s \tau) \mathcal{U}_{\mathcal{I}}^s (\tau \mathcal{U}_{\mathcal{I}}^s \tau))$.

b) for $b > a$ in each summation of the elements of rows to derive the below inequality

$$\begin{aligned}
& \sum_{t=1}^n f_0(t) + \sum_{t=1}^n f_1(t) + \dots + \sum_{t=1}^n f_l(t) > \\
& n + \frac{n(n+1)}{2} + \frac{2^n - 1}{2 - 1} + \frac{3^n - 1}{3 - 1} + \dots + \frac{l^n - 1}{l - 1} > \\
& n + \frac{n(n+1)}{2} + 2^{(n-1)} + 3^{(n-1)} + \dots + l^{(n-1)} \\
& \quad - (1 + \frac{1}{2} + \frac{1}{3} + \dots + \frac{1}{l-1}) \\
& \quad > 2^{(n-1)} + 3^{(n-1)} + \dots + l^{(n-1)}
\end{aligned}$$

where $n \geq 2$. Therefore, we have

$$\sum_{t=1}^n f_0(t) + \sum_{t=1}^n f_1(t) + \dots + \sum_{t=1}^n f_l(t) > l^{(n-1)} \quad (25)$$

This concludes the complexity of the algorithm to be $\Omega(|\varphi_s|^{(|\hat{\rho}|-1)})$.

C. A Polynomial Time/Space Fragment of STPL

In the following, we assume that the size of the spatial formula φ_s is bounded.

1) *Example:* The complexities of evaluating an arbitrary SPE formula φ_s (the formula is in conjunctive form) on a data stream $\hat{\rho}$ is

- $O(2^a 3^b)$ for time and space, if there is no complement operator in the formula, where $a, b \in \mathbb{N}$, and we have: $\text{argmax}(2^a 3^b \mid (|\varphi_s| + 1)/2 = 2a + 3b)$. For instance, $\varphi_s := (\mathcal{T} \sqcup \mathcal{T} \sqcup \mathcal{T}) \sqcap (\mathcal{T} \sqcup \mathcal{T} \sqcup \mathcal{T})$.
- $O(4^{((|\varphi_s|+1)/3)})$ for time and space, if there are complement operators in the NNF formula. For instance, $\varphi_s := \bar{\mathcal{T}} \sqcap \bar{\mathcal{T}} \sqcap \bar{\mathcal{T}} \sqcap \bar{\mathcal{T}} \sqcap \bar{\mathcal{T}} \sqcap \bar{\mathcal{T}}$.

2) *Example:* An arbitrary l -level nesting spatial globally formula φ_s^\square , with a spatial term as its right-most subformula, is of $O(|\hat{\rho}|)$ time and $O(1)$ space complexity.

$$\varphi_s^\square := \square_{\mathcal{I}}^s \left(\mathcal{T} \sqcap \square_{\mathcal{I}}^s \left(\mathcal{T} \sqcap \square_{\mathcal{I}}^s \left(\mathcal{T} \sqcap \square_{\mathcal{I}}^s \mathcal{T} \right) \right) \right)$$

3) *Example:* An arbitrary l -level nesting spatial eventually formula φ_s^\diamond , with a spatial term as its right-most subformula, is of $O(|\hat{\rho}|^{(l+1)})$ time and space complexity.

$$\varphi_s^\diamond := \diamond_{\mathcal{I}}^s \left(\mathcal{T} \sqcup \diamond_{\mathcal{I}}^s \left(\mathcal{T} \sqcup \diamond_{\mathcal{I}}^s \left(\mathcal{T} \sqcup \diamond_{\mathcal{I}}^s \mathcal{T} \right) \right) \right)$$

4) *Example:* An arbitrary l -level nesting spatial eventually subformula φ_s^\diamond followed by an arbitrary k -level nesting spatial globally subformula φ_s^\square , with a spatial term as its right-most subformula, is of $O(|\hat{\rho}|^{(l+1)})$ time and space complexity.

$$\varphi_s^{\diamond, \square} := \diamond_{\mathcal{I}}^s \left(\mathcal{T} \sqcup \diamond_{\mathcal{I}}^s \left(\mathcal{T} \sqcup \diamond_{\mathcal{I}}^s \left(\mathcal{T} \sqcup \diamond_{\mathcal{I}}^s \left(\square_{\mathcal{I}}^s \left(\mathcal{T} \sqcap \square_{\mathcal{I}}^s \left(\mathcal{T} \sqcap \square_{\mathcal{I}}^s \mathcal{T} \right) \right) \right) \right) \right) \right)$$

5) *Example:* A right-hand-side l -level nesting spatial until formula $\varphi_s^{\mathcal{U}}$, where the left-hand-side of all the until operators are a single spatial term, is of $O(|\hat{\rho}|^{(l+2)})$.

$$\varphi_s^{\mathcal{U}} := \mathcal{T} \mathcal{U}_{\mathcal{I}}^s \left(\mathcal{T} \mathcal{U}_{\mathcal{I}}^s \left(\mathcal{T} \mathcal{U}_{\mathcal{I}}^s \left(\mathcal{T} \mathcal{U}_{\mathcal{I}}^s \mathcal{T} \right) \right) \right)$$

6) *Example:* A left-hand-side l -level nesting spatial release formula $\varphi_s^{\mathcal{R}}$, where the right-hand-side of all the until operators are a single spatial term, is of $O(|\hat{\rho}|^{(l+2)})$.

$$\varphi_s^{\mathcal{R}} := \left(\left(\left(\mathcal{T} \mathcal{R}_{\mathcal{I}}^s \mathcal{T} \right) \mathcal{R}_{\mathcal{I}}^s \mathcal{T} \right) \mathcal{R}_{\mathcal{I}}^s \mathcal{T} \right) \mathcal{R}_{\mathcal{I}}^s \mathcal{T}$$